

GEOOTHERMOMETRIC STUDIES ON THE ATTEPE IRON DEPOSITS

Ali Rıza ÇOLAKOĞLU* and Gülay SEZERER KURU*

ABSTRACT.- This study was carried out in the Attepe (Yahyalı) iron mineralization zone of Kayseri province. The main mineralization zone is 500 m long and lies approximately in the NNW/SSE direction. The study covers the geothermometric analyses which were carried out on the fluid inclusions of siderite, quartz and barites in relation within the iron mineralization. In this study samples were taken from five different rock groups observed in the field and were evaluated as a, b, c, d, e. Four different fluid inclusion types were determined in the siderite, quartz and barites of these rock groups (type I, type II, type III and type IV fluid inclusions). As a result of these studies three different formation processes were determined within the ore mineralization zone, namely (1) early stage, (2) late stage and (3) final late stage. Homogenization temperatures were 300-350°C in the early stage, 180-270°C in the late stage and 170-250°C in the final late stage. Early stage first group quartzes have in average 43 % NaCl in the early stage, the late stage quartzes of the first group on average have 35 % NaCl and the final stage barites have 3 % NaCl equivalent salinity. According to the macro observations in the mineralization area and the homogenization temperature measurements made in laboratory whatever the origin of the fluids, the deposits were formed in the hydrothermal stage conditions and hypothermal, mesothermal and epithermal stages were active in these hydrothermal stages.

INTRODUCTION

The region within the Attepe iron mine which covers the study area is the second largest iron basin of Turkey. This deposit is described firstly as Faras mine by Lucius in the year 1972. In the region, The first comprehensive studies on ore deposits were started in the year 1967. After this period, studies have been carried out by various researchers and the region were investigated in detail in the terms of regional geology and ore deposits. First geologic studies dealing with the chronostratigraphy were done by Blumenthal (1944) and Abdüsselamoğlu (1958). Most detailed petrographical, geochemical, genetical and ore microscopy studies in the terms of mineralization were done by Küpeli, (1986, 1991 and 1999); Ayhan et al., (1992). Other detailed studies dealing with regional geology

and mineralization are also present (Ayhan and İplikçi, 1980; Metin 1983; Henden et al., 1978; Henden and Önder, 1980; Önder and Şahin, 1979, Şahin and Bakırdağ, 1985; Dağlıoğlu, 1990; Dağlıoğlu and Bançeci, 1992; Dağlıoğlu et al., 1998). This region is very important for steel-iron sector in our country that ore production has been going on since 1969.

Mineralogical, petrographical and geochemical studies have revealed that the iron ores in Attepe and its vicinity were present in three different genetic types (Küpeli, 1986; 1991; Dağlıoğlu et al., 1998). In the region, mineralizations have been seen in the units which are of Mesozoic, Lower-Middle Cambrian, and Lower Cambrian ages (Dağlıoğlu et al., 1998; Küpeli, 1999). These are sedimentary pyrite and hematite occurrences (type, I),

hydrothermal siderite and hematite occurrences (type, II), and karstic iron ores occurrences (type, III). Pyrite and hematite occurrences (type, I), in the Lower Cambrian aged bituminous shale-phyllite and metaquartzites which are deposited in the sedimentary type are firstly described by (Küpelı, 1986). The argument that the II'nd. type mineralization in the Lower-Middle Cambrian aged metacarbonates formed as a result of the hydrothermal processes are accepted by the all researchers except Unlu and Stendal (1986). Based on the geochemical data Ünlü and Stendal (1986) suggest a sedimentary model (Küpelı, 1999). The II'nd type mineralization were formed in the Paleocene-Lower Eocene time periods on the other hand the III'rd type mineralization are formed at the beginning of Tertiary epoch, by storage in endokarstic holes in the form of secondary ironhydroxide group of minerals within the framework of terrestrial movements and karstic processes of multiple phases (Küpelı, 1991). The most important mineralizations in the region are classified as type II and type III ores.

Mineralization have developed in tectonically controlled form and found as veins, lenses and irregularly shaped masses. Pyrite, tetrahedrite, chalcopyrite, marcasite, siderite, barite and little hematite and magnetite are observed as ore minerals in all of these type mineralizations (Küpelı, 1999). In order to determine the conditions of the mineralization process and for the purpose of clarifying the previous observations and conclusions, geothermometric measurements were made on samples of five characters (a, b, c, d, e) in the field studies (fig. 1). In this study siderite, quartz and barite in connection with the mineralization zones are evaluated. The purpose

of these geothermometric measurement studies" were the determination of the homogenization temperatures of these minerals and the determination of the fluid inclusion types developed in connection with the mineralization processes, attempts were also made to obtain new data to support the previous data and to determine the formation processes of the ore deposits.

GEOLOGICAL SETTING

The Attepe iron ore deposits are bounded by Geyikdağı unit, considered as ootocyon by Özgül (1976), in the south, by Aladağ unit in the west, by Kireçliyayla melange in the north and by Göksun metamorphics in the east. The oldest rocks of this region within this area are the Sicimindağ formation of Geyikdağı unit. This formation contains Attepe member on the top which is formed by alternating bituminous schist, phyllite and shales and Kandilcikdere member at the bottom composed of schist and phyllite metquartzites (fig. 1). On top of this formation lies the Çaltepe formation of Lower-Middle Cambrian age (Dean and Monod, 1970). On top of these formations lies the Seydişehir formation of Upper Cambrian and Ordovician age containing Elmadağı ve Eğrisöğütödalı members and the unit is composed of calcschist, phyllite, limestone with nodules and metasandstones. On top of these formations the Karakızıođlu formation of Mesozoic age are present with an angular discordance. It is composed of schist, phyllite calcschist and recrystallized limestones. The mineralization is observed as lense and vein shaped in all formations older than the Miocene age. The most important mineralization are observed in metacarbonates of Lower-Middle Cambrian age (fig. 1).

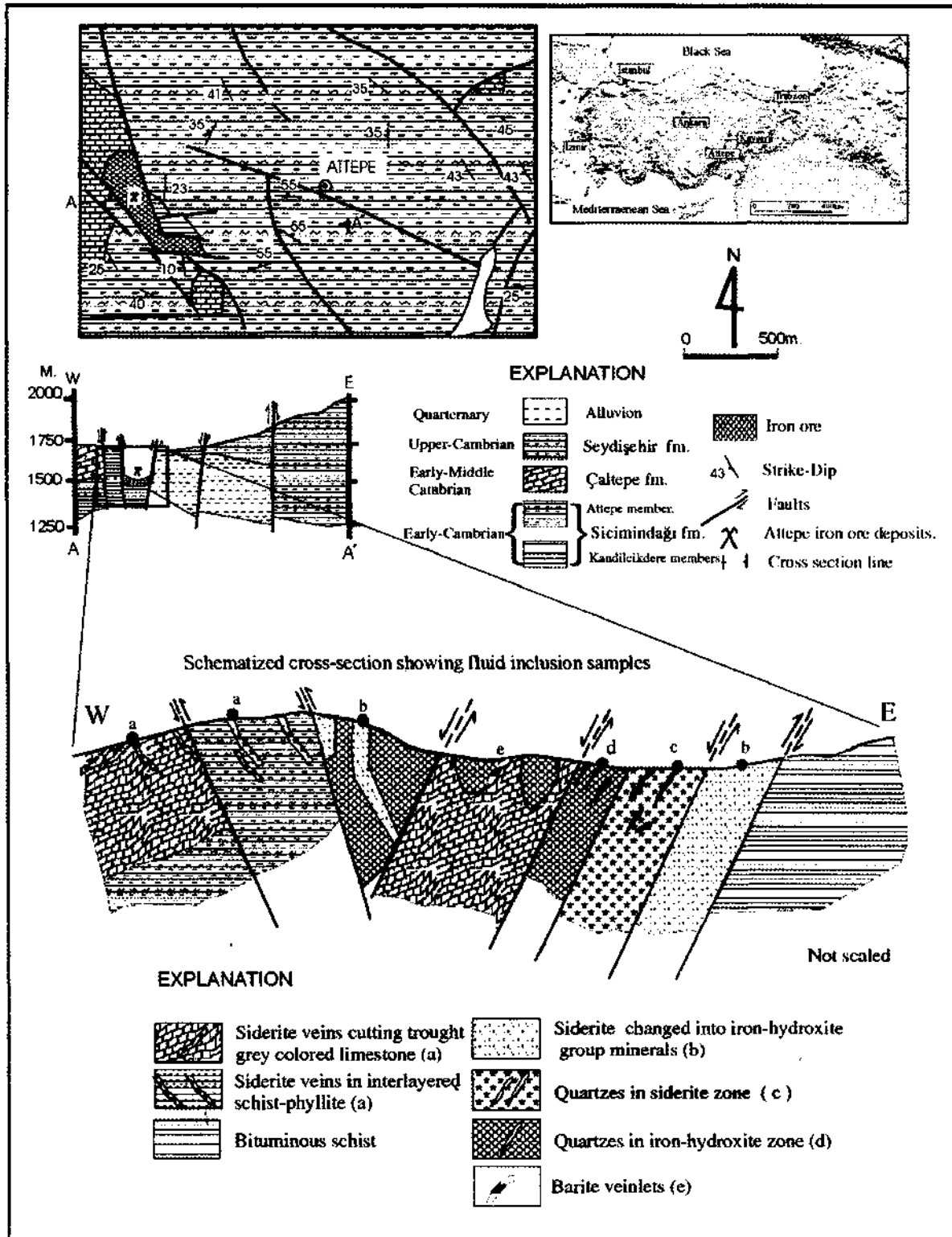


Fig. 1- Schematic cross-section view showing the sample types and geological map of the investigation area. (Modified after Ayhan et al., 1992).

FLUID INCLUSION PETROGRAPHY

Samples are taken from the quarry operated by open-pit method for studies of fluid inclusion. These samples are, (a) siderite veins cutting through grey colored limestones, (b) light brown-dark brown colored siderite transformed into iron-hydroxite group minerals, (c) quartzes found in siderite and partly cutting through it, (d) quartzes in iron-hydroxite zone and (e) less observed barite seen in the mineralization zone.

Fluid inclusions which are classified into four groups in are further subgrouped into five group samples (fig. 2). According to the composition and fluid inclusions in the samples (a, b, c, d, e) are grouped into four different groups (Roedder, 1984):

Type I. fluid inclusions: two phases (liquid + vapor).

Type II. fluid inclusions: three phases (liquid + vapor + solid).

Type III. fluid inclusions: one phases (liquid).

Type IV. fluid inclusions: one phase (vapor).

As a result of the studies similar types of fluid inclusions were differentiated into primary and secondary origins however only the data from the fluid inclusions of primary type were evaluated.

Dimensions of these fluid inclusions of four types are generally within 2-18 microns. They provide different fluid inclusion types with regular and irregular forms morphologies. For example in siderites fluid inclusions of type I and II, in quartzites types I, II, III and IV; and in barites only type I fluid inclusion is observed.

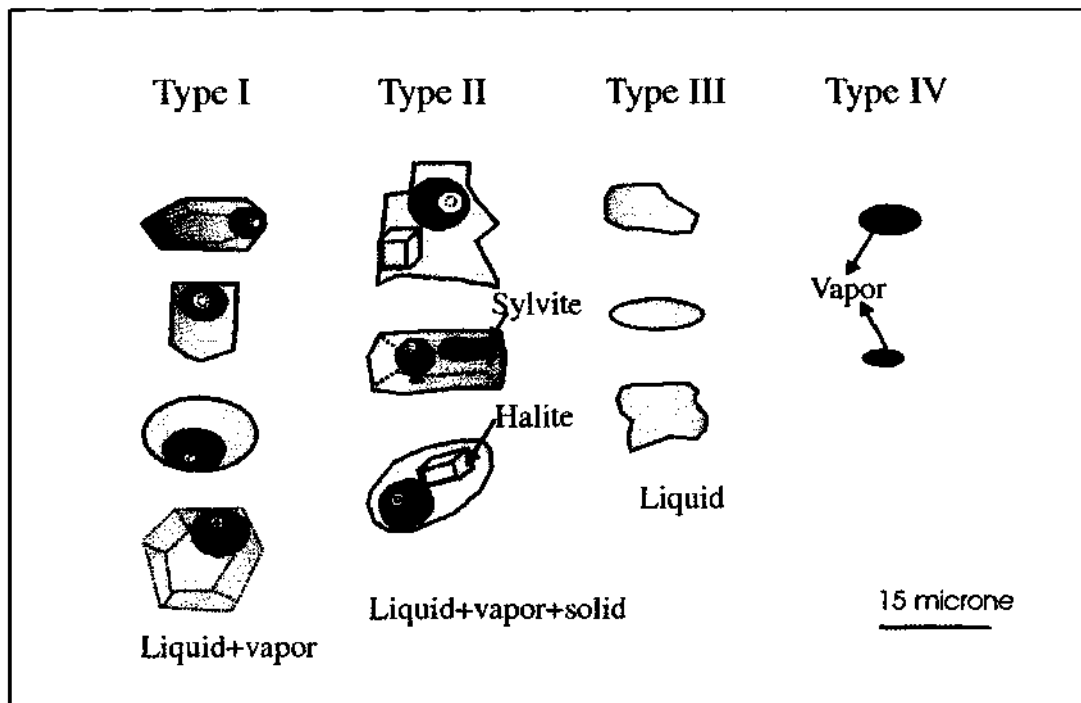


Fig. 2- Fluid inclusion types observed in siderite, quartz and barite in Attepe iron ore deposits.

Geothermometric studies

Geothermometric measurements are made according to the USGS fluid inclusion systems. During the heating and freezing measurements liquid and gaseous nitrogen is used. The instrument is calibrated as $\pm 0,2^{\circ}\text{C}$ for temperatures below 0°C and as $\pm 2,0^{\circ}\text{C}$ for higher temperatures. Synthetic fluid inclusions containing CO_2 and liquid phases are used in the calibration. To prevent the spoiling

of the primary characteristics of the fluid inclusions by heat cold adhesives (entallan) is used and two sides are polished and 35 micron thick special fluid inclusion sections are produced. Results of geothermometric measurements made on the fluid inclusions of siderite, quartz and barites taken from the mineral phases related to the ore are given in summary form (Table-1).

Table 1- The properties of fluid inclusion In mineral forming fluid

Sample Type	Type	Stage	The melting temperature daughter minerals	Dimenson microne	Salinity Wt % NaCl	Mean	Frequency	Homogenization Temperature Interval	Mean
Second group siderite	Type I	Stage 1		2-18			12	180-290	236
Second group siderite	Type I	Stage 2		2-18			8	310-370	336
First group quartz	Type I	Stage 1		3-16			16	180-270	214
First group quartz	Type I	Stage 2		3-16			20	300-450	371
First group quartz	Type II	Stage 1	(-23,4/-53,7)*	3-16	31-38	35	18	170-280	235
First group quartz	Type II	Stage 2		3-16	40-45	43	34	300-440	375
Second group quartz	Type I	Stage I		4-18			37	180-350	256
Barite	Type I	Stage I	(-3,1/-4,8)	2-18	2,7-3,2	3	15	170-250	213

Siderites

Lenses of siderite are usually of 10-80 cm thickness. In some locations siderites are in the form of crack fills. Siderites are divided into two groupes. First groups of siderite form siderite veins cross cutting to grey colored limestones and schist rocks (a), second group of siderites are of light dark brown colored. These are siderites (b) which show wide scale spreading compared to the first group of siderites and gradually inserted into ironhydroxide group of minerals

First group of siderites (a) have--relatively small crystals (0.1-0.3 mm) and the siderites in this group were not taken into account since sufficient data is not obtained during the geothermometric measurements because

they have very few fluid inclusions. The second group of siderites have larger crystals (0.3 mm to 1 cm) and they contain few amounts of type I fluid inclusions of 6-10 microns dimensions. Homogenization temperatures obtained from the heating experiments made on these fluid inclusions indicate two separate phases. In the first stage the homogeneza-tion temperatures are in between 180-290°C. In the second stage the homogeneza-tion temperatures are in between 310-370°C (fig. 3). During the freezing experiments as the melting points were not properly observed a clear melting point temperature interval could not be given. For this reason the salinity values of this type fluid inclusions could not be determined.

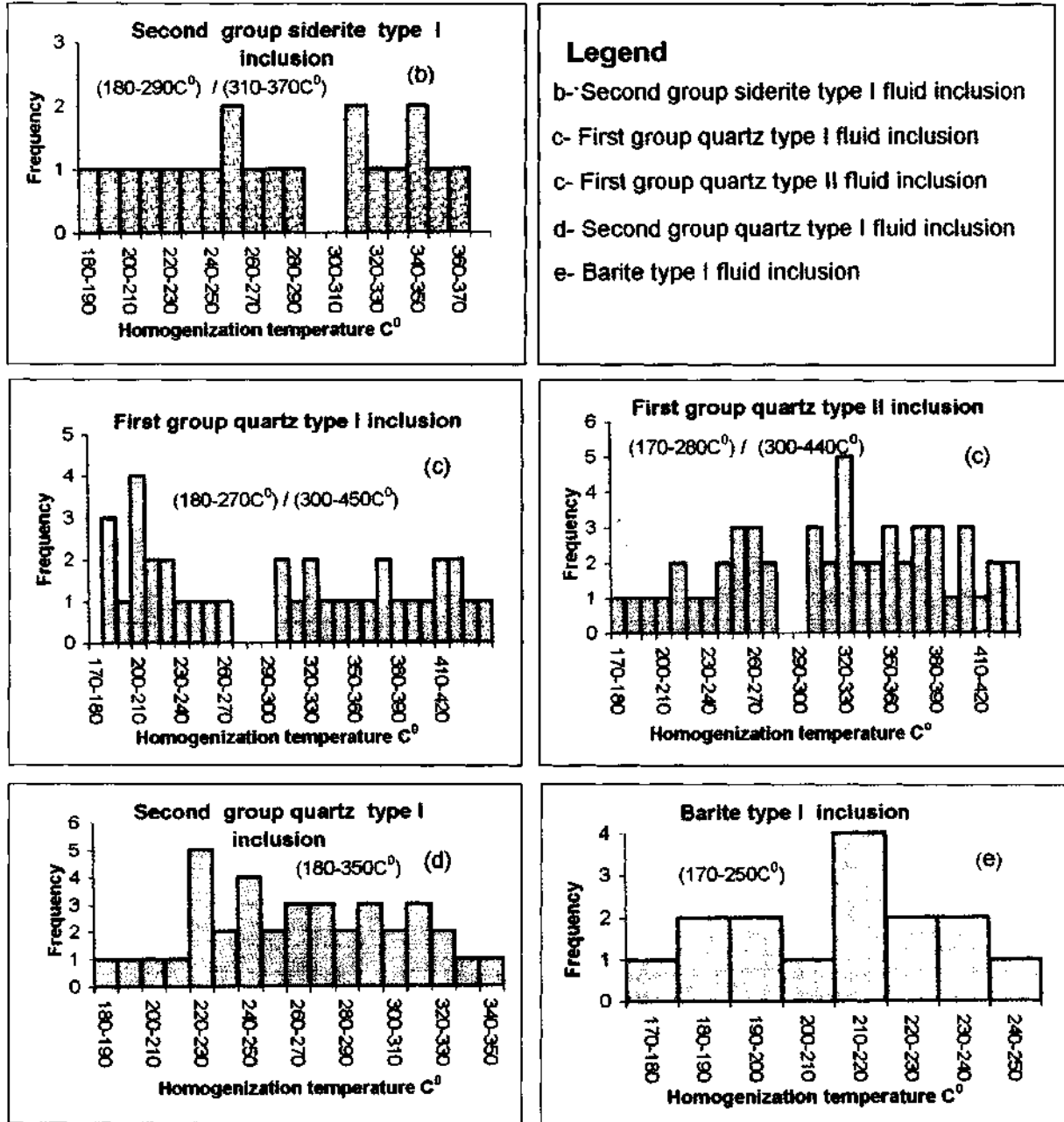


Fig. 3- The homogenization temperatures measured from siderite, quartz and barite in Attepe iron ore deposits.

Quartzes

Quartzes are investigated in two different groups. The first group of quartzes, are the kind of quartzes which are observed together with siderites. They also contain pseudomorphic pyrites transformed into ironhydroxide group of minerals (c). Quartzites are present in the mineral phases related to the above mentioned minerals and are observed in siderites in the form of stockwork and vein type structures. In other words they form the gang mineral within the ore mineral zone. Fluid inclusions of types I., II., III. and IV. are observed in these veins. The dimensions of fluid inclusions vary from 3 to 16 microns. Homogenization temperatures of I'st type fluid inclusions of first group quartzites indicate two different stages. In the first stage the homogenization temperatures are in between 180-270°C, in the second stage it is in, between 300-450°C (fig. 3). Homogenization temperatures of II'nd type of fluid inclusions of first group of quartzes also indicate to distinct stages. Homogenization temperature of the first stage are in between 170-280°C, in the second stage it is in between 300-440°C (fig. 3). Simultaneous observation of fluid inclusions of types MI and IV in quartzes indicates the occurrence of boiling event. For this reason no pressure correction was applied to the homogenization temperatures measured from the geothermometric measurements.

It is observed that solid phases (daughter crystals) of some of the II'nd type fluid inclusions of first group quartzites did not melt at temperatures higher than 450°C while some of the daughter crystals of the same type of fluid inclusions melted before the disappearance of the fluid inclusion bubble. In

the heating tests the daughter crystals of silvite melts at higher temperatures than halite crystals (Roeder, 1984). Thus it is considered that in this study the crystals which had melted before the disappearance of the bubble is halite and the others, that is those daughter crystals which had not melted at higher temperatures is silvite. The melting temperatures of daughter crystals (for halites) of II'nd type of fluid inclusions varies between 23.4-53.7°C. By consideration of these melting temperatures it is determined that the salinity of this type of fluid inclusion is equivalent to % 31-45 NaCl. From these salinity values the equivalent NaCl for the first stage is % 31-38, and for the second stage % 40-45. For the first group of quartzes geothermometric measurement result of type I and II fluid inclusion indicate similarities.

The second group of quartzites are those quartzites which are coincident with the ironhydroxide group of minerals and which cross them (d). Among them only the I'st type of fluid inclusions is observed. The dimensions of this type of fluid inclusions vary from 4 to 18 microns and show high inconsistency. The presence of high inconsistency behaviour of fluid inclusions makes the performance of the freezing tests on fluid inclusions difficult. The homogenization temperatures obtained from the heating tests of I'st type of fluid inclusions of second group of, quartzites are dispersed between 180-350°C and the most frequently observed homogenization temperatures are 220-320°C (Refer to fig.3).

Barites

Barites are encountered stratigraphically in the upper levels of the all the iron ore

outcrops in the Mansurlu region. Due to the removal of cover layers of barites are rarely encountered in the ore zones. The presence of barites in stratigraphic order necessitates the geothermometric studies in the barites. Barites have larger crystals and are more transparent as compared to other minerals. Among the barites type I fluid inclusions of 2-18 micron dimensions and generally with regular dimensions are encountered. As a result of the geothermometric measurement studies homogenization temperatures varying from 170 to 250°C are determined (Refer to fig. 3). As a result of freezing tests equivalent salinity values of % 2,5-2,7 NaCl are determined. The considerably low homogenization temperature values of barites indicate that they are formed in a rather late epoch. It is known that the barites characterize the medium and the low temperature minerals in the hydrothermal siderite veins (Mondadori, 1990).

THE ORE AND GANGUE MINERALOGY AND PARAGENESIS

Within the study area siderite, hematite and pyrite are observed as the most frequent ore minerals while barites are scarcely observed. Gangue minerals are seen generally as quartz and calcite. Among these minerals siderites, quartzites and barites are used in the fluid inclusion measurements. While the measurements made from the first group of quartzite inclusions of types I and II (c) indicate a two phased temperature interval, the fluid inclusions of second group of quartzites (type I) give a single phase interval. In the second group of siderites a temperature phase similar to the first group quartzites had developed (Refer to fig. 3).

Based on the fluid inclusion results three distinct formation processes were determined in the region. These are, (1) early phase formations (first group of quartzites of having type I. and II. fluid inclusions, second group of quartzites having I'st type of fluid inclusions and second group of siderites having I'st. type of fluid inclusions), (2) late phase formations (first group of quartzites having I'st and IInd. type of fluid inclusions, and second group of siderites having I'st type of fluid inclusions) and (3) final late stage formations (barites of type I fluid inclusions) (fig.4).

Homogenization temperatures are determined as 300-350°C in the early stage and 180-270°C and 170-250°C in the late and final late stages respectively. The equivalent salinity of the first group of quartzites formed in the early stage is % 43 NaCl while the salinity for late stage is % 35 on the average It is determined that the barites formed in the final late stage, having fluid inclusions of type I have equivalent salinity of % 3 NaCl. The fact that the initially high and later low salinity values can be explained by the possibility that meteoric water mixing into the solutions (fig. 4). In the vein type of deposits after the formation of the first quartzite occurs which plaster the crack, a temperature increase in the vein is observed (Akıncı 1976). Most probably, this temperature rise creates a model which is in agreement with the hydrothermal thesis and it probably caused the decreases in the degree of salinity and temperature values in the time in which by the inclusion of meteoric waters (fig. 4).

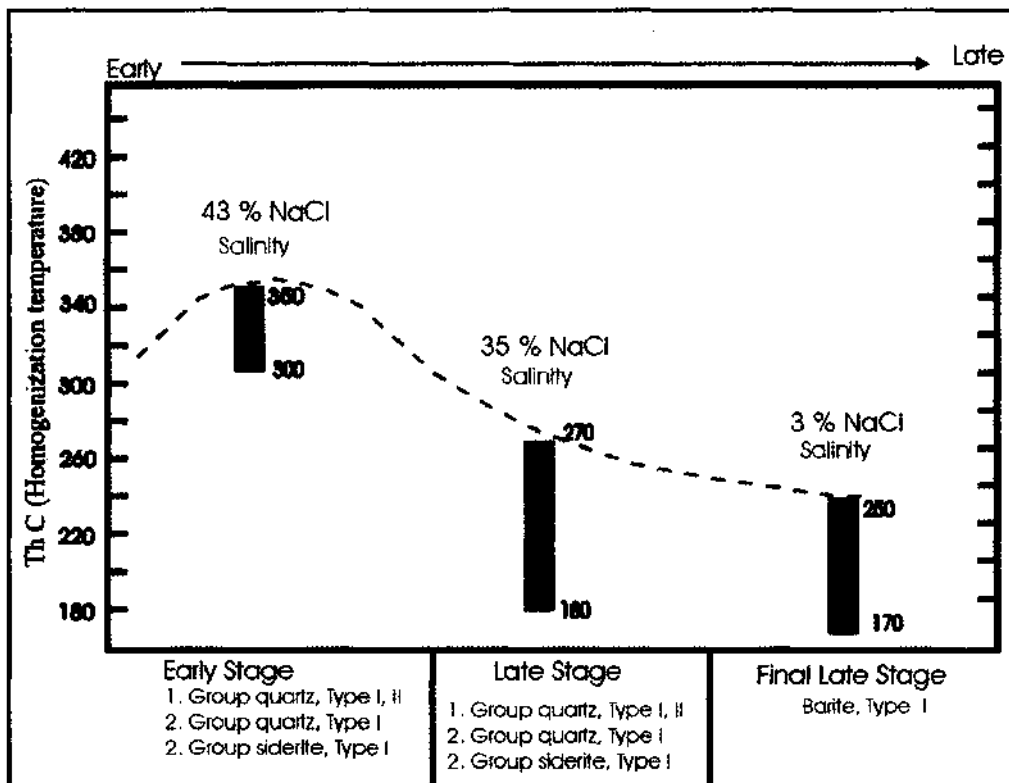


Fig. 4- The main temperature stages of ore and gangue minerals in Attepe iron deposit.

RESULTS AND DISCUSSION

Attepe iron deposit and the neighbouring iron mineralization that have been formed in three different genetic types have been reported by the previous studies (Küpelı, 1986; 1991; Dağlıođlu and et al, 1998). These are sedimentary pyrite and hematite occurrences (type, I), hydrothermal siderite and hematite occurrences (type, II) and karstic iron ores (type III). The argument that the ores of type II were formed as a result of hydrothermal processes within the Lower-Middle Cambrian aged metacarbonates are accepted by all investigators except Ünlü and Stendal (1986). In this study in order to support these views, studies of fluid inclusions were performed. By

means of the study of geothermometric measurements in the fluid inclusions present in the samples (a, b, c, d, e) taken from the mineralization zone, four different type of fluid inclusions are determined. The dimensions of these fluid inclusions are generally in the range of 2 to 18 microns. As a result, different types of fluid inclusions that have regular and irregular shaped morphologic structure were observed. Since siderites in the first group (a) have small crystals (0.1-0.3 mm) and there were insufficient data due to less fluid inclusions in the geothermometric measuring studies, siderites in these groups were assumed to be negligible (since not considered), only second group of siderites have been evaluated.

Therefore, considering the geothermometric measurement on siderite, quartz and barite content at Attepe iron mineralization, the quartzes with I. and II. type fluid inclusions and the siderites with I. type fluid inclusions represent same type homogenization heat intervals (Table 1).

Based on the geothermometric measurement results three different formation processes were determined for the region. These are: (1) early phase formations (first group of quartzites of having type I. and II. fluid inclusions, second group of quartzites having I st type of fluid inclusion and second group of siderites having I st. type of fluid inclusions), (2) late phase formations (first group of quartzites having I st and II nd. type of fluid inclusions, and second group of siderites having I st type of fluid inclusions) and (3) final late stage formations (barites of type I fluid inclusions) (fig. 4).

Homogenization temperatures are determined as 300-350°C for the early stage and 180-270°C and 170-250°C in the late and final late stages respectively. The equivalent salinity of the first groupe of quartzites having type II fluid inclusions, formed in the early stage is %43 NaCl, while the salinity for late stage is on the average %35. It is determined that the barites having type I fluid inclusions formed in the final late stage have equivalent salinity of %3 NaCl. Simultaneous observation of type III and IV fluid inclusions indicates boiling event. For this reason no pressure correction were applied to the homogenization temperatures measured from the geothermometric measurements.

The mineralization in the region took place at homogenization temperatures of 300-350°C (early stage) and 180-270°C (late stage) in acidic and in reductive conditions, in the

solution system of NaCl + KCl + H₂O with high salinity. The conditions of this formation process matches the mesothermal and hypothermal stages of hydrothermal stage (Lindgren 1933). It is known that waters of magmatic origin as well as the waters of meteoric origin were influential in the conditions of the formation process (Roedder, 1984). With the further decrease of the temperature (170-250°C) and the salinity (approximately %3 NaCl equivalent salinity) of the environment in the final late stage formation of barites are added to the NaCl + H₂O solution system. These formation conditions represent the final periods of epithermal stages of the hydrothermal stages and the mesothermal stages (Lindgren 1933). The decrease of the high temperature and salinity values of the early stage indicate the probable mixing of meteoric waters into the environment in the final late stage.

Finally "hydrothermal thesis" for genetic types of II and III are supported.

Manuscript received January 28, 2002

REFERENCES

- Abdusselamogiu, Ş., 1958, Yukarı Seyhan Bölgesinde Doğu Toroslar'ın jeolojik etüdü: MTA Rep. 2668, Ankara, 38s (unpublished), Ankara.
- Akıncı, Ö.T., 1976, Bulancak guneyindeki sülfid damarlarında sıvı kapanım çalışması. TJK Bülteni, 19, 45-52.
- Ayhan, A. and İplikçi, E., 1980, Adana iline bağlı Kozan-Feke-Saimbeyli dolayının jeoloji Raporu. MTA Derleme No: 6737.
- , Küpeli, Ş. and Amstutz. G.C., 1992, Attepe (Feke-Adana) demir yatağının bitişindeki pirit oluşumları. MTA Dergisi 111, s. 85-94.
- Blumenthal, M. M., 1944, Kayseri-Malatya arasındaki Toros'un Permo Karboniferi: MTA Dergisi, 31, 1, 105-133.

- Dağlıoğlu, C., 1990, Mansurlu yöresi TDÇI sahalarında yapılan etüt ve arama çalışmaları raporu. MTA Rep. 8910 (unpublished), Ankara.
- and Bahçeci, A., 1992, Adana-Feke-Mansurlu TDÇI ruhsat sahalarının (Attepe, Koruyeri (Mağrabeli) değerlendirme raporu: MTA Genel Müdürlüğü Derleme No: 9339 (unpublished), Ankara.
- ; ——— and Akça, I. 1998, Attepe, Koruyeri (Mağrabeli), Hanyeri batısı (TDÇI Genel Müdürlüğüne ait) demir madenlerinin değerlendirme raporu: MTA Genel Müdürlüğü Rep. 2823 (unpublished), Ankara.
- Dean, WT., and Monod, O., 1970, The Lower Paleozoic stratigraphy and faunas of the Taurus Mountains near Beyşehir, Turkey: I. Stratigraphy Bull. Brit. Mus. (Nat. Hist.) Geol., 19, 8, 411-426.
- Henden, I.; Önder, E.; and Yurt, M.Z., 1978, Adana-Kayseri-Mansurlu-Karköy-Attepe-Elmadağbeli-Kizilmevkii - Menteşdere-Uyuzpınarı demir madenleri jeoloji ve rezerv raporu: MTA Genel Müdürlüğü, Rep. 6394 (unpublished), Ankara.
- and ———, 1980, Attepe (mansurlu) demir madeninin Jeolojisi, T.J.K Bülteni, 23, 153-163.
- Küpeli, S., 1986, Attepe (Mansurlu) yöresinin demir yatakları: Selçuk Üniversitesi Fen Bilimleri Enstitüsü, Yüksek Lisans Tezi, Konya, 111s. (unpublished).
- , 1991, Attepe (Mansurlu-Feke) yöresi ve demir yataklarının jeolojik-petrografik ve jenetik incelenmesi: Selçuk Üniversitesi, Fen Bilimleri Enstitüsü, Doktora Tezi, 227s. (unpublished).
- , 1999, Attepe (Mansurlu-Feke-Adana) demir yatağı ile yakın çevresindeki cevher oluşum tipleri ve bazı jeokimyasal özellikleri: Yerbilimleri Geosound, sayı: 34, s. 247-271.
- Lindgren, W., 1933, Mineral deposits. 4th edition New York: Mc Graw-Hill. 930p.
- Lucius, M., 1972, Antitoros silsilesinde Zamanti suyu ve Göksu arasında Faraş demir madeni zuhurunda yapılan jeolojik rapor. MTA Genel Müdürlüğü Rep. 421 (unpublished), Ankara.
- Mondadori, A., 1990, The Mcdonald encyclopedia of rocks and minerals: Mcdonald and Co (Publishers) Ltd., Spain, 607 s.
- Metin, S., 1983, Doğu Toroslarda Derebaşı (Dereli) Armutalan ve Gedikli (Saimbeyli) köyleri arasının jeolojisi. İstanbul Üniversitesi Mühendislik Fakültesi Yerbilimleri Dergisi c: 4 Sayı:1-2.
- Önder, E., and Şahin, M., 1979, Adana-Feke-Mansurlu (Hanyeri, Çaldağ, Taşlık Tepe, Bahçecik, Çandırlar, Kısacıklı) demir sahaları jeoloji ve Kozan, Saimbeyli ilçeleri prospeksiyon raporu. MTA Maden Etüt Arşiv Raporu No: 1636 (unpublished).
- Özgül, N., 1976, Torosların bazı temel jeolojik özellikleri: TJK Bülteni c:19 s.1, 65-78.
- Roedder, E., 1984. Reviews in Mineralogy, Fluid Inclusions Mineralogical Society of America, 644p.
- Şahin, M., and Bakırdağ, L., 1985, Kayseri-Adana, Yahyalı-Delialıuşağı-Karakızoluğu, Feke-Mansurlu-Karakızoluğu Gediği, Mağrabeli (Güney bölüm), Hanyeri demir madeni jeoloji ve rezerv raporu. MTA Genel Müdürlüğü Derleme No:6394 (unpublished).
- Ünlü, T., and Stendal, H., 1986, Divriği bölgesi demir yataklarının element korelasyonu ve jeokimyası (Orta Anadolu Türkiye): Jeoloji Mühendisliği Odası Dergisi, 28, 5-19.

DEPOSITIONAL ENVIRONMENTS AND PETROGRAPHY OF DENİZLİ TRAVERTINES

Mehmet ÖZKUL*, Baki VAROL** and M. Cihat ALÇİÇEK*

ABSTRACT- Quaternary to Recent travertines in the Denizli basin are distinguished in 9 lithofacies according to the field and microscobic features. These are: 1) Crystalline crust, 2) Shrub, 3) Pisolith, 4) Paper-thin raft, 5) Coated gas bubble, 6) Reed, 7) Lithoclast, 8) Pebbly travertines and 9) Palaeosols. Various combinations of the distinguished lithofacies are deposited on slope, depression, mound, fissure ridge and channel depositional environments. In addition, these main depositional environments are divided into subenvironments. As to isotope analysis made of some travertine samples, $\delta^{13}\text{C}$ and $\delta^{18}\text{O}$ values show a wide distribution. The $\delta^{13}\text{C}$ values are between 0.35‰ and 6.70‰; $\delta^{18}\text{O}$ values are -6.47‰ to -15.10 ‰. Consequently, an isotopic grouping have been brought up based on lithofacies variation and depositional environments.

INTRODUCTION

The Denizli basin is an important region in sense of travertine formation both in Turkey and the world. A part from modern Pamukkale travertines where a lot of tourists visit every year, there are extensive travertine masses at different parts of the basin, especially along the northern margin (fig. 1). The total area occupied by modern and old travertines is more than 100 km² in the basin and their thickness is up to 60 m (fig. 2). Some of the old travertines have been quarrying by marble industry for a long time.

Travertines are limestones that form where hot ground waters, rich in calcium and bicarbonate, emerge at springs (Guo and Riding, 1998). CO₂ outgassing causes rapid travertine precipitation. Travertines have a complex internal architecture frequently changing both in lateral and vertical directions in short distance. This complexity is originated from many factors such as spring position, underlying topography, chemical composition of travertine depositing waters, organic activity and surfacial waters. Recently, there are increase in the studies made on geochemistry, morphological types, macro- and microorganic components, stable isotope variations and dating of travertines both in Turkey and the world (i.e. Chafetz and Folk-1984; Pentecost and Tortora, 1989; Guo and

Riding, 1998, 1999; Guo et al., 1996; Srdoc et al., 1989, 1994). Most of the studies made on the Denizli travertines are generally focused on Pamukkale and related to hydrogeology of the hot waters, geothermal potential, wasting and conversation. (Koçak, 1971; Şentürk et al., 1971; Canik, 1978; Eşder and Yılmaz, 1991; Gökgöz, 1994; Gökgöz and Filiz, 1998; Ekmekçi et al., 1995). Some studies have been subjected the stratigraphical position of travertines in the basin, dating, morphological classification, relations between travertine and neotectonics-seismicity of the region (Altunel and Hancock, 1993 *a,b* and Altunel, 1996), travertine geochemistry and physico-mechanical features (Demirkıran and Çalap-kulu, 2001 and Özpınar et al., 2001). In the previous works, depositional features (lithotypes, facies, etc.), organic and inorganic components, petrography of the travertines have not been sufficiently investigated. Phototrophic microorganisms, their distribution and influence on the travertine deposition investigated by Pentecost et al. (1997) are only confined modern Pamukkale travertines. Aim of this study is to describe the different lithofacies of recent and old travertines in the basin context, according to field and petrographical features and to determine environments where the lithofacies have precipitated. In addition, some stable isotope variations were studied.

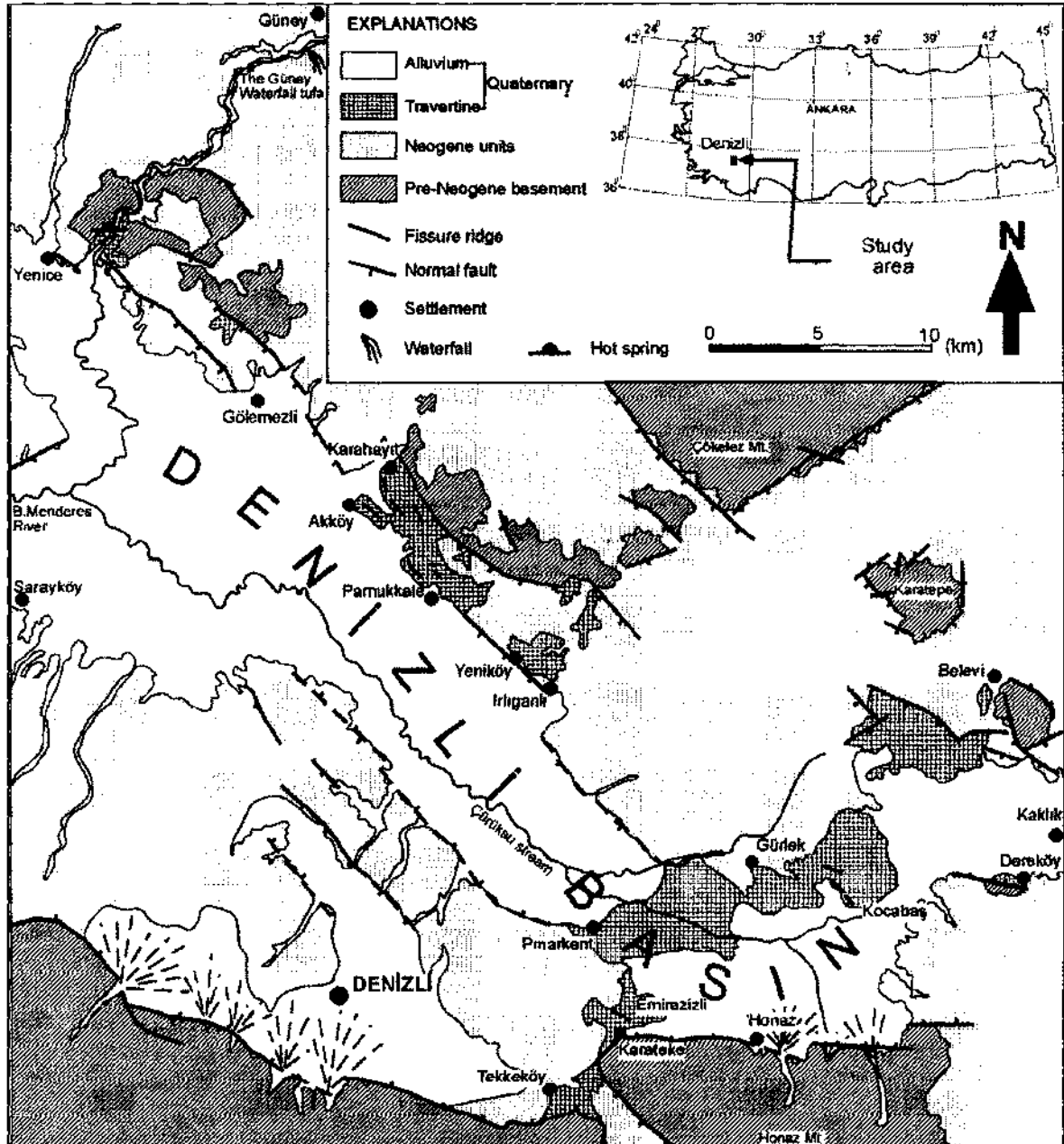


Fig. 1- Simplified geological map of the Denizli basin and distribution of main travertine masses (modified from Sun, 1990).

GEOLOGICAL SETTING

The depression 50 km long, 25 km wide located at the eastern end of junction locality where Büyük Menderes and Gediz grabens was named as Denizli basin (Westaway,

1990, 1993). Pre-Neogene basement rocks of the basin that crop out at the horst areas are consisted of metamorphic rocks of Menderes massif represented schist, marble and allochthonous Mesozoic carbonates

and ophiolites and Paleogene limestone, dolomite and evaporites. The basin filled by Neogene-Quaternary deposits was bounded by normal faults both in the north and south margins (Fig. 1). The Neogene sequence, which are deposited lake and river environments and Late Miocene (Meotian-Pontian) in age (as ascribed by Taner, 2001), exposes commonly at the basin margins and some uplifted areas in the middle. The basin extends in NE-SW direction. According to Westaway (1993), the extension has begun in the Middle Miocene (ca 14 Ma. ago). Travertine masses in the Denizli basin have deposited where dip-slip normal fault segments display step over along strike (Çakır, 1999). The spring waters take required ions from the basement carbonate rocks for the travertine accumulation. The travertines deposited by emerging waters along the extensional fissures and normal faults rest on the Neogene sediments. Travertines at the quarries to the northwest of Kaklık (Fig. 1) are transitional in lateral and vertical directions with greenish gray, cream-coloured lake-marsh deposits, reddish-brown coloured alluvium, palaeosol and coarse-grained ephemeral river sediments (Fig. 2). Travertines in this region have gained a stepped structure from north to south by normal faulting series. Nevertheless, age of first travertine accumulation in the basin have not been clarified yet, the oldest travertines at Pamukkale are at least 400.000 years in age, as pointed out by Altunel (1996). During our study, some vertebrata teeth and jaws were found at the travertine quarries to the northwest of Kaklık. By the preliminary description, it has been found out that these vertebrata bones belong to Equus, who is an ancestor of modern horse in Quaternary (Ş. Şen and G. Saraç, 2001; personal communication).

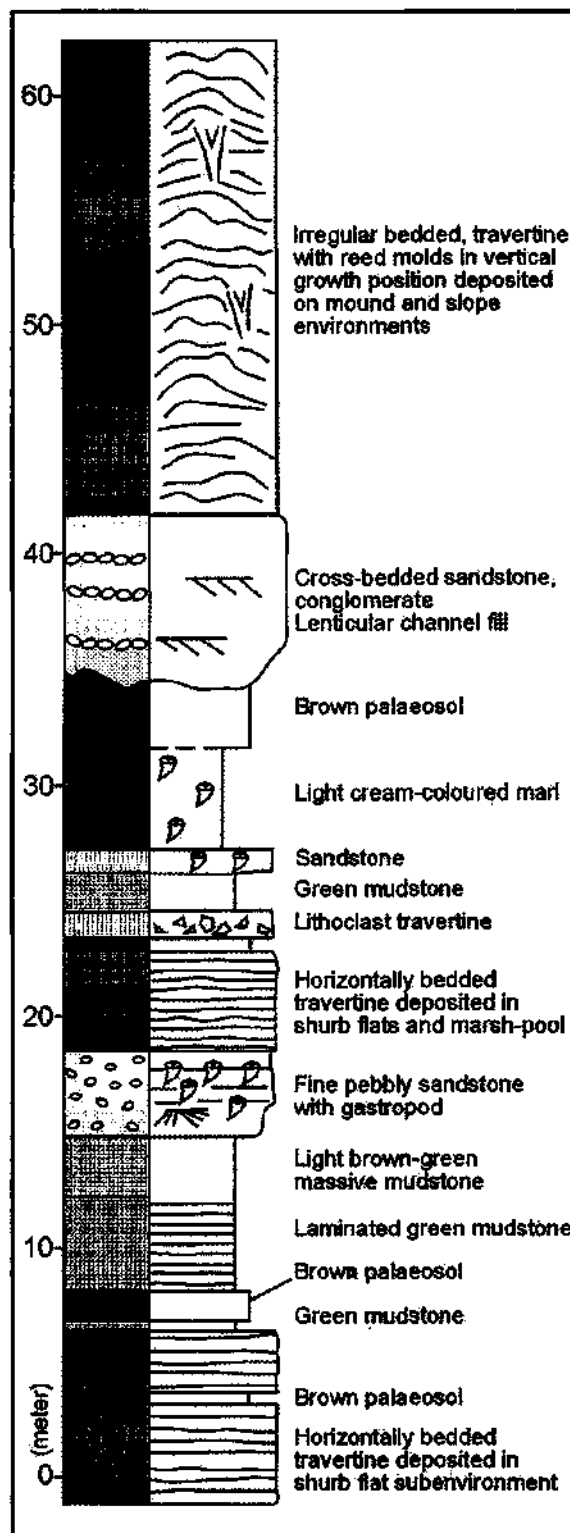


Fig. 2- Measured stratigraphical section at travertines located at the northwest Kaklık (The İlik quarry, southern slope of the Killiktepe).

METHODS

Samples are collected from the different travertine lithofacies, by investigating the field properties. SEM analysis of the collected samples were made by using Jeol JSM-840 type electron microscope in the Turkish Petroleum Corporation Laboratory, Ankara. In order to perform that, polished surfaces of the rock samples were etched by %5 HCl during 3-5 seconds and then coated by gold in a vacuum system, the images were taken. Stable isotope analyses were made at the Isotope Laboratory of Tübingen University.

PETROGRAPHY OF THE DENİZLİ TRAVERTINES

Travertines precipitated at different depositional conditions display variations of colour, appearance, bedding, porosity, texture, and composition. In this study, different travertine precipitates in the Denizli basin were separated into the lithofacies based on field scale and petrographical features of the samples taken from each lithofacies were investigated.

Mainly travertine lithofacies: 1) Crystalline crust, 2) Shrub, 3) Pisolith, 4), Paper-thin raft, 5) Coated gas bubble, 6) Reed, 7) Lithoclast and 8) Pebbly travertine. Paleosol horizons (9) are formations that point out erosion and nondeposition periods and frequently coincided with travertine sequences.

1) Crystalline crust travertine lithofacies

Crystalline crust travertines (Guo and Riding, 1992, 1998) commonly form as a result of rapid precipitation from fast flowing waters on smooth slope, rims and vertical walls of terrace pools, cliff surface of waterfall subenvironments and in extensional fissures (fig. 3). Crystalline crusts are commonly dense, crudely fibrous, light-coloured, consisting of elongated calcite feathers, developed perpendicular to the depositional surface. The crystalline crusts change from a few centimeters to meter in thickness. The outer

crust surfaces are usually ornamented by microterrace pools.

Previously, the vertical crystalline crusts developed in the extensional fissure ridges at Pamukkale were named as banded travertines by Altunel and Hancock (1993a) and Altunel (1996). Crystals in the banded structure are perpendicular to the vertical fissure walls of which depositional surfaces. By reason of that, the banded travertines precipitated along the vertical walls of extensional fissures (Plate I, fig. 1) also have been accepted as crystalline crust travertines in this study. These vertical banded crusts filling the fissure space display slower and entirely inorganic precipitation by degassing of CO₂. Crusts at the Kamara hot spring in the Büyük Menderes valley to the northwest of the Denizli basin and at Karahayıt near Pamukkale are consisted of alternation of white, red, and brown colour layers due to high iron content of the hot spring waters. Guo and Riding (1998) determined that old crystalline crusts were compact and hard, but when young, as at Terme San Giovanni, near Rapolano Terme, Italy, they can be delicate and easily crushed.

In the microscopic appearances, it is seen that micrit and sparit laminae are alternated (Plate I, fig. 2). The micritic laminae commonly are dark-coloured and in millimetric scale. In dark micritic laminae, the solution pores have developed in places. The sparite laminae, which are centimeter and decimeter in scale, may contain iron of various ratio. The spar crystals have grown radially on the micritic basement and organised as bundles in some places. Better development of one side of the crystals gives a cedar tree appearance (Plate I, fig. 3) (Folk et al., 1985). These crystals that are 10 micron in width and 100-200 micron in length are distinguished with the smooth crystal boundaries from each others. In addition to unfractured crystals, fractured pieces are also fairly abundant. The

fractured crystals are seen as a fill of the interspaces or randomly distributed in a micritic floor (Plate II, fig.1, 2). In SEM images, calcite crystals forming the crust display blade edge like appearances (Plate II, fig.1, 2).

Due to high flow velocity of water, the crystalline crust develops where biogenic activity is limited (Guo and Riding, 1998). Formation of the radial calcite crystals is a result of direct crystallization from hot water. Any trace reflecting the microbial activity is not coincided with the microscopic appearances of the samples. The alternation of light and dark layers have been interpreted as diurnal variation near spring area (Folk et al., 1985; Guo and Riding, 1998).

2) Shrub travertine lithofacies

Travertines represented by small bush-like growths are common deposits on horizontal-subhorizontal surfaces (Chafetz and Folk, 1984; Guo and Riding, 1994, 1998 and Chafetz and Guidry, 1999). They are bounded by the micritic layers from both bottom and top. The shrub lithofacies is the most common one in the Denizli travertines. Individual shrub layers in the macro samples are light cream-coloured, 3-16 mm in thickness and seen as irregular horizons (Plate I, fig. 4).

Under the microscope, they are composed of the crystal associations of spar and micrite organized in different ways. In general, there is not a clear boundary between two kinds of crystal shapes. In thin sections, prepared perpendicular to the bedding, the spaces among the dark-coloured micritic shrub forms that expand upward were filled by secondary spar calcite mosaic (Plate I, fig. 5). Whereas, in the thin sections, parallel or slightly oblique to the bedding, dark micritic clumps in the sparite constitute a mottled texture as islands or patches. The densely and loosely packed micritic fields can be separated in the shrub samples. Completely micritic

fields are observed where the shrub forms have densely packed. The densely packed shrubs consist of euhedral and subhedral crystals, 5-10 μm in size, without having any internal architecture. These have been commonly found in the shrub formations in mixed with spar crystals.

Loosely packed micrites, in the form of thin levels in places, comprise abundant diatoms (Plate III, fig. 1). The micritic clumps are very common in the mottled texture and form the structures resembling bubble and pustule (Plate III, fig. 8). The cloudy micrites have developed on the spar crystals. They compose of the micritic grains that are 5-15 μm in size and wholly unihedral. In addition, the rod-shaped micrite crystals and calcified tubes are found within them (Plate II, fig. 3). The spar crystals followed in the form of residue under the micritic clumps support that those areas have become sparmicritization. Kahle (1977) has described this event as micritization forming by dissolution-crystallization in spar crystals from the way of biotic and abiotic. In the samples, the bacterial filaments that is widely seen in the fields where the sparmicritization is present, supporting the micrite has a biogenic origin.

According to Guo and Riding (1994, 1998), shrub forms are ordinary components of terrace pools, but the shrubs in layers are the most common and the thickest lithofacies of shrub flats (shallow, extensive pools) and subsequently marsh-like environments in depressions and on low angle slopes (fig. 3). In the studied travertines, the shrubs display transitions to the crystalline crust, reed, paper-thin raft and irregular radial pisoliths (bacterially mediated). According to Chafetz and Folk (1984), shrub layers represent growing season (spring-summer), whereas micritic layers represent the non-growing season (winter). Bacterial shrubs formed from heated waters, i.e., water temperatures were above

ambient water temperatures for a region (Chafetz and Guidry, 1999). For this reason, shrub forms are not observed in cool water travertines (=tufas). Abiotic origin was also proposed for shrubs (Pentecost, 1990). This kind of shrubs display needle crystal shrubs' of Guo and Riding (1994) and 'crystal shrubs' and 'ray crystal shrubs' of Chafetz and Guidry (1999).

3) Pisolith travertine lithofacies

Coated grains as pisoliths are common in travertines. (Chafetz and Meredith, 1983; Folk and Chafetz, 1983 and Guo and Riding, 1998). Pisoliths form in small terrace pools of the steep slopes, and wide pools in depression fields (fig. 3). In addition, pisoliths were found in the self-built channels of Pamukkale during this study. Pisoliths occurred in the wide pools are generally associated with shrub form and micritic carbonate. Grain shape ranges from spherical to discoidal, in control of water agitation and microbial activity (Folk and Chafetz, 1983). Previously, three types of pisoliths are distinguished based on texture: 1) Concentrically laminated (Folk and Chafetz, 1983), 2) Radial shrub (Folk and Chafetz, 1983) and 3) Stromatolitic mammillated (Guo, 1993).

First two types are observed in the Denizli travertines. Concentrically laminated pisoliths were originated from splashing and turbulent water in terrace pools and self-built channels. The grains size of spherical particles are up to a few cm (Plate I, fig. 6). Although their nuclei are always not clear, they have usually grown on a dark micritic nuclei. Crystals forming the nucleus are coarser (10-15 mm) than those in thin micritic layers of the pisolith microstructure (Plate III, fig. 6). The thin micritic layers that cover the radial calcite crystals are entirely ksenotopic, consisted of grains of 3-6 mm in size. There are interfaces that have restricted the growth in pisolith microstructure. The interfaces are

microkarstification and dissolution structures that do not show lateral continuity (Plate III, fig. 2, 3) and also transform into a microstromatolitic structure in some places. The microkarstification and dissolution structures point out most probably desiccation periods in the terrace pools. Concentrically laminated pisoliths have been accepted to be inorganic (Folk and Chafetz, 1983).

4) Raft travertine lithofacies

The rafts are thin, delicate and brittle crystalline layers precipitated at the water surfaces of pools and main fissure apertures filled by hot waters of the travertine ridges (Plate I, fig., 7, 8). They are composed of calcite and/or aragonite crystals and their extend quietly limited, in meter scale. Present day rafts are going on to precipitate at the water surfaces of the pools located both on terraced steep slope and near the hot spring orifices at Pamukkale and Karahayıt respectively. Dense raft concentrations are commonly associated with coated gas bubbles at the Çukurbağ hot spring (Plate IV, fig. 8), of which temperature is 58°C. The colours of the rafts range from white to brown, based on chemical composition of the hot water. The horizontal rafts occurred in the main fissure of an old travertine ridge near the Kocabaş, village (Plate IV, fig. 7) are associated with lithoclasts and vertical crystalline crusts (Plate I, fig. 7). The old examples of the rafts are thickened a little due to secondary encrustation in early diagenetic stage, as exemplified by Guo and Riding (1998) from Rapolano Terme, Italy. Previously, the rafts are named as 'hot water ice' (Allen ve Day, 1935), 'calcite ice' (Bargar, 1978), 'calcite rafts' (Folk et al., 1985) and 'paper-thin rafts' (Guo and Riding, 1998). The Similar occurrences are also well known from cool water cave pools (Baker and Frostick, 1951; Black, 1953).

5) Coated bubble travertine lithofacies

The coated gas bubbles are common in depositional environments of travertine such as terrace pools and extensive equivalents in the depressions. The origin of the gas bubbles is microbiologic activity in the base sediments of the pools. They are mainly trapped beneath the paper-thin rafts, among the plants and in the crystals and preserved by rapidly coating by calcium carbonate. Therefore, the coated gas bubbles are usually observed together with the crystalline crust, raft (Plate I, fig. 8) and reed travertine lithofacies. The shape of the bubbles is spherical and oblate and their sizes range from millimeter to centimeter. Guo and Riding (1998) pointed out that some coated bubbles have gained a tubular appearance by joining each other. Chafetz and Folk (1984) have termed the coated bubbles as 'lithified bubbles' and 'foam rock'. Coated bubbles have a similar structure to that of paper-thin raft with an inner micritic layer and an outer (water side) veneer of euhedral, mainly aragonite crystals. The bimineralic wall structure has been attributed to variation in supersaturation level of the water (Chafetz et al., 1991 a).

6) Reed travertine lithofacies

Reed lithofacies are one of the prominent elements in the Denizli travertines deposited marsh-pool, mound and self-built channels. The travertines rich in molds of reed and coarse grass were named 'reed travertine' by Guo (1993) and Guo and Riding (1998). Reed, grass and similar water plant grow in distal areas where hot spring waters cool and dilute due to rain influence. The plant clusters obstacles the water flow and the roots stabilize the sediments and encrusted mostly by micritic carbonate. The remaining spaces from the plants were partly or entirely, filled by the same material. The cylindrical molds up to 2-3 cm wide. The calcite crystals of 20-150 mm that have form from space wall to the center are typical. The reed lithofacies

is usually associated with the rafts. The reed travertine lithofacies are ordinary component of both marsh-like shallow depressions drying time to time and reed mound. The organic matter content and pore ratio of the reed travertine are much more than the others lithofacies. The lithofacies is seen at the upper levels of the quarries located to the northwest of Kaklık town.

7) Lithoclast travertine lithofacies

Lithoclasts are penecontemporaneous, angular to subangular travertine fragments in different size, by erosion of the upper slopes and collapse of waterfalls and terrace cliffs. The fragments derived from the slope are commonly light-coloured. The fragments are subsequently deposited at the lower slope and in the depressions. In addition, more locally, some fragments broken off from the upper part of fissure walls have fallen down into the fissure apertures (Plate I, fig. 7). The dark-coloured lithoclast interlayers in the horizontal travertines that have deposited in the shrub-flat and marsh-pool subenvironments of the depressions is 20-100 cm in thickness. This lithoclast interlayers show pedogenic alteration and caliche formation at the lower and upper parts. The brecciation, colour and texture variation are common in the lithoclast travertine lithofacies that has been observed locally.

8) Pebbly travertine lithofacies

Some travertines investigated in the Denizli basin contain sparse rounded pebbles of limestone, marble, chert, radiolarit and serpentinite. The pebbly travertines are seen around the antique tombs between Küçükdere and Irlıganlı villages and some quarry fields located to the northwest of Kaklık. In addition, they have been observed as dropped down pebbles into the fissure spaces of the ridges. These rounded pebbles in the travertines have probably derived by the ephemeral floodings from the basement

units of Neogene and the older sedimentary rocks adjacent to the travertine depositional environments. The pebbly travertine lithofacies described here may be partly correlated with 'cemented rudites' recognized in the British travertines by Pentecost (1993).

9) Palaeosol lithofacies

Decrease in water supply and diversion in flow direction result rapid exposure of travertine surface to rain water, subaerial desiccation, biological activities and soil formation. Although palaeosol formation is not directly a travertine lithofacies, closely related to the travertines precipitated especially in depressions and lower slopes. The palaeosol interbeds in the Denizli travertines are frequently seen at the quarries to the northwest of Kaklık. In the sequence logged at one of these quarries, four different brown-coloured palaeosol interbeds were separated ranging from 40 cm to 3 m in thickness (fig. 2). The bed thickness increases from the slope to the depressions. The each palaeosol bed has constituted a sequence boundary between the two travertines. The thickness of palaeosol is related to how long the travertine is exposed.

TRAVERTINE DEPOSITIONAL ENVIRONMENTS

The lithofacies described above have been represented in state of various combinations in different depositional environments. They are found mainly three depositional environments: 1) Slope depositional environment, 2) Depression depositional environment; 3) Mound depositional environments. This kind of classification was previously made at the Rapolano Terme hot spring travertines (Italy) by Guo and Riding (1998).

In addition to the three environments explained above, two additional main types of depositional environments were also defined in this study. One of them is fissure ridge formed by emerging hot waters along the

extensional fractures and the other self-built channel called fourth and fifth depositional environment respectively.

1. Slope Depositional Environment

Slope depositional environment are divided into three subenvironment:

a) Terraced slope, b) Smooth slope and c) Waterfall.

a) Terraced slope subenvironment.- The most spectacular and present day examples of the slope environment are formed at Pamukkale (Plate IV, fig. 1). The terrace pools are developed on the slope morphology. The terraced slopes consist of vertical terrace walls, pools and rims confining the margins of the pools. The vertical terrace walls and rims are composed of crystalline crust lithofacies. Paper-thin rafts, pisoliths and coated gas bubbles are the additional lithofacies formed at the base of pools. The terrace pools occur on the prograding slope where waters flow turbulent.

b) Smooth slope subenvironment.- The smooth slope forms where the slope dips are between 10-40°, on which the terrace pools have not developed. The recent smooth slope subenvironments at Pamukkale are transitional with terraced slope both in vertical and lateral direction (Plate IV, fig. 1). The dominant lithotype precipitating on the smooth slope is crystalline crust as seen on the walls and rims of the terrace pools. The thickness of crust is range from centimeter to a few decimeters. Feather crystals forming the crusts are perpendicular to the slope surface. Smooth slopes develop where waters usually flow in laminar. Thicker crystalline crusts represent rapid deposition under high flow rates whereas thinner crust precipitated by slower flow (Folk et al., 1985; Guo and Riding, 1998). But thin crystalline crusts were deposited by alternating with shrub layers on the low-angled slope where water supply and flow velocity are low. Thin lithoclast levels are even observed at lower parts of slope.

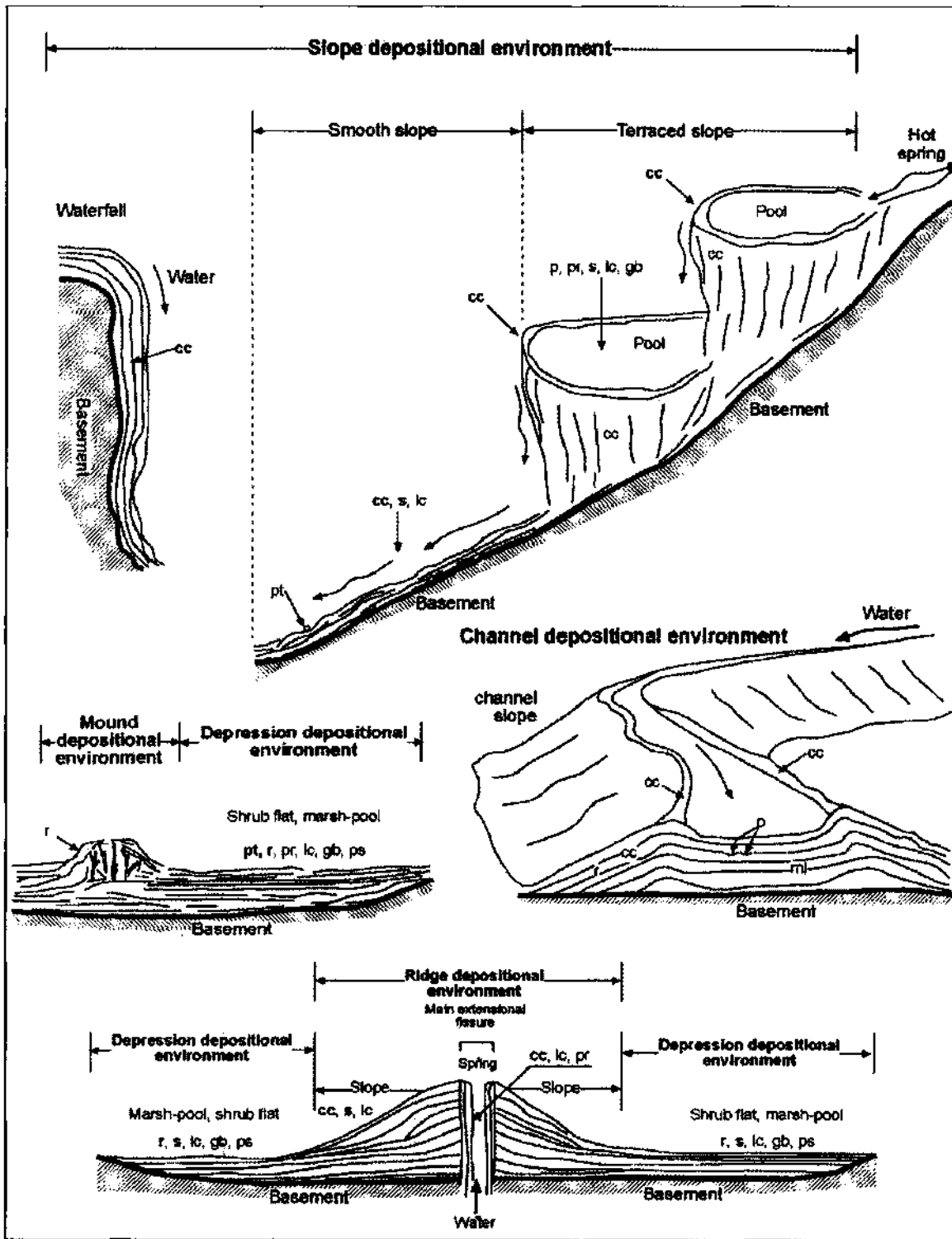


Fig.3 - Depositional environment and subenvironments of travertine lithofacies. cc: crystalline crust, s: shrub, p: pisolith, pr: paper-thin raft, gb: coated gas bubble, r: reed, lc: lithoclast, pt: pebbly travertine, ps: palaeosol, ml: micritic laminae, Bold letters indicate the dominant lithofacies.

c) Waterfall subenvironment- The waterfall subenvironment is much more local and restricted than the others. An active waterfall is located at the left slope of B. Menderes river valley, three kilometers south of Güney town in the northwest of Denizli (fig. 1). It is forming by cool spring waters of 16°-18°C. Therefore, these porous travertines are considered as tufa that calcium carbonate encrusts the plants. At the same locality there are inactive counterparts.

A second inactive example has been formed on the steep slope facing to the north of Keltepe, along a fault scarp, near Dereköy (fig. 1). The waterfall travertines are deposited on a vertical substrata, resembling an overhanged curtain (Plate IV, fig. 3). The overhanged deposits have been mainly composed of crystalline crusts. The waterfall travertines have been passed into the smooth slope at the lower altitudes in the time, towards north.

2- Depression depositional environment

These kinds of depositional environments have been introduced during the studies made on Rapolano Terme travertines locating south of Florence, Italy (Guo, 1993; Guo and Riding, 1998). They are flats and hallows in areas of relatively low topography and divided into two subenvironments: a) Shrub flat, b) Marsh-pool. The depression depositional environments are located in front of the slopes and around of the fissure ridges (Plate IV, fig. 8).

a) Shrub flat subenvironment- Shrub flats are subenvironments in which the horizontal and subhorizontal, travertines have deposited. The travertines deposited in these environments are light-coloured, thin-bedded laterally extensive and consist of mainly shrub lithofacies (Plate IV, Fig. 5,6). The shrub flat travertines comprise some lithoclast interbeds. Long-term erosion periods and short-term precipitation interruptions result

palaeosols and desiccation surfaces respectively. In addition, red mudstones and conglomerates interpreted as products of floodings and ephemeral streams are associated with the shrub travertines (fig. 2). In the studied area, lower parts of the quarries in Belevi and northwestern of Kaklık (Killiktepe and just north of the Denizli Cement Factory) composed of the travertines of shrub flat subenvironments (Plate IV, fig. 4,5,6). Transitions from the shrub flats to marsh-pools subenvironments are represented by alternation of light and dark coloured layers in a travertine unit as seen on the wire-cut surfaces (Plate IV, fig. 6).

At the bottom of the Alimoğlu quarry located to the southern slope of the Killiktepe, a shrub flat travertine unit is up to 5 m thick. The thickness of 5 m at the north decreases to 2.5 m in distance of 90 m. In the same direction, the colour is become darker laterally. The unit are underlain by a brown palaeosol bed and overlain by gray, green-coloured thin mudstone deposited in the marsh. In the other quarry near Alimoğlu, four different travertine units have been observed from the bottom to the top, which are precipitated in the shrub flat subenvironments (fig. 2). Their thicknesses change between 1.5 and 5 m.

b) Marsh-pool subenvironment. - Dominant rock types of the marshpool subenvironments are horizontal, gray, brown-coloured travertines that are rich in reed lithofacies. The marsh-pool deposits are interbedded with light-coloured travertines of the shrub flat subenvironments and transitional in lateral direction. They comprise lithoclastic interlayers and common pedogenic indications. Gastropod tests are locally abundant. The travertines near Kocabaş village deposited in the marsh-pool subenvironments of the depressions located around the fissure ridges have not been sufficiently consolidated yet. These are darker and more porous relative to the slope travertines. Therefore, we think that

Kocabaş mass is younger than the travertines at the quarries in the north, four km far from there.

On the other hand, these types of travertines that are widespread at the Honaz, Karateke, Pınarkent and Gürlek areas have formed a plateau stepped from the south to the north (fig. 1). The travertines of these areas are darker, more porous, rich in organic content, with high pedogenic effects and reed appearance in lithofacies and much more in tufa character. On the road cuts between the railway and the highway near Pınarkent, angular travertine lithoclasts in different sizes eroded from southern part of the plateau were redeposited as colluvium on a slope surface of 25-30°.

3- Mound depositional environment

Reed mound depositional environment are those that the water plants densely located in depressions and near lower slopes. The travertines of this environments have been previously introduced as 'mound depositional system' and its reed mound fades by Guo and Riding (1998). In the studied area, travertines of the mound environments have developed in association with the horizontally bedded travertines of shrub flat and marsh-pool subenvironments belonging to the depressions, at the upper parts of the quarries both around Killiktepe and just north of the Denizli Cement Factory in the northwest of Kaklık (fig. 2). The most prominent deposits of the environment is reed travertine lithofacies. The reed clusters in the growth position expand upward. At the slopes of the mound, the beds dip away from the crest with angles of 10°-35°. The subsequent lithofacies such as micritic laminae, paper-thin rafts and coated gas bubbles are accompanied by the reed travertines. Some voids of the reeds were filled by micritic laminae and paper-thin rafts.

4- Fissure-ridge depositional environment

Fissure ridges (Bargar, 1978) are narrow linear mounds formed where hot spring waters emerge along a joint or fault on an elevation (Guo and Riding 1998). Fissure ridges entirely have diverse depositional morphology relative to the slope environments. In the Denizli basin, both active and inactive examples of the fissure ridges are observed (Altunel and Hancock, 1993a; Altunel, 1996; Çakır, 1999; Özkul and Alçiçek, 2000; Özkul et al., 2001). The fissure ridges at Pamukkale and Kocabaş have been investigated earlier in neotectonic and seismic aspects (Altunel and Hancock, 1993 a, b). According to Çakır (1999), fissure ridges occurred along the northwest margin of the basin are preferentially developed at the ends of the normal fault segments or in step-over zones between them. The most fissures are parallel to the faults, but some are oblique. Although the ridges are located along the northwest margin of the basin, there are a few examples occurred near the southern margin and in central parts, as is well seen at the west end of the Honaz fault (Bozkuş et al., 2000) and around Kocabaş respectively. B. Menderes valley (near Yenice), Gölemezli, Pamukkale-Karahayıt, Akköy, Kocabaş and Honaz are main locations where the ridge morphologies are observed completely or partly, (fig. 1; Plate IV, fig. 7 and 8).

Both the Kamara ridge in the valley of Büyük Menderes river and the Kırmızısu fissure ridge near Karahayıt are active and all the others inactive. The ridges seen straight or sinuous in plan view are 100-1400 m long, up to 20 m high and 20-125 m wide at the base. The width of individual fissures is maximum in the middle and become narrow towards both terminations. Fissure width of east-west trending Kuşgözü ridge is 7 m in the middle, 5 m in the western end, at the northwest of Kocabaş village (Plate IV, fig. 7). Vertically banded crystalline crust lithofacies

are precipitated on the walls of fissures that the hot waters emerge (Plate I, fig. 1), The crystalline crusts in some fissure fills are associated with coarse-grained lithoclasts and crystal rafts and coated gas bubbles (Plate I, fig. 7). The fissure space that the hot water does not emerge are filled by red palaeosol, angular travertine lithoclasts, and gravels.

On the both slopes of the ridges, the bedded travertines are deposited in flanking away from the main ridge axes. The dips of the bedded travertines range from almost vertical to 5°. The terrace pools in macro- and microscales have been formed on some ridge slopes. The inclined travertine layers on the fissure slopes include almost all the travertine lithofacies. The most prominent lithofacies are micritic laminae, crystalline crust, shrub, rafts, and lithoclast. The lithoclasts have been resulted by both erosion of the upper slopes near the crest and repeating extensional fracturing in time. The inclined layers distally pass into the adjacent flats and depressions around the ridges (Plate IV, fig. 8). The facies in the fissure slopes rapidly changes in short distances, even a few meters. Rapid facies variations in short distance are typical feature for fissure ridges (Guo and Riding, 1999).

5- Self-built channel depositional environment

Self-built channels are linear travertine masses built up by spring waters in flow direction. Active and inactive examples of the channels are common in Pamukkale and around Kocabaş. The inactive channels are partly destroyed, eroded and collapsed in places due to human activities and natural processes, such as earthquake shaking, as seen in Pamukkale (Altunel, 1994). The channel formation are realized either by natural process or man-made for irrigation. Marginal slopes range from vertical to flanking surfaces. Morphologic and structural properties and distribution of them have been previously investigated by Altunel (1994) and Altunel and Hancock (1993a). They have sinuous

shape in plan view and cut-cone or 'M'-shaped (term of Altunel and Hancock, 1993a) in cross section. The channel thalweg are restricted by rims from the both sides. The - rims have developed along the points where precipitation is maximum, similar to those that in the terrace pools.

The self-built channels show lithofacies variations in a short distance as well as the fissure ridges and the terraced slopes. The channel thalweg grow as gradually upward in time by alternation of micritic laminae and crystalline crusts. The pisolith clumps observed in some hollows placed along the thalweg are formed by agitated water. At the same time, the channel slopes are developed in small scale on the both sides by overflowing and splashing water. The slopes are composed of inclined crystalline crusts, thin micritic layers and reed lithofacies. The combinations and the ratios of the lithofacies change from place to place along the channels.

STABLE ISOTOPES

Oxygen and carbon stable isotope analyses were performed on the nine samples of the Denizli travertines. $\delta^{13}\text{C}$ isotope values changes between 0.35 and 6.7 ‰ while $\delta^{18}\text{O}$ values varies from -6.47 to -15.10 ‰ (Table 1). Groundwater isotopic characteristics are modified in case of water emerging from spring. Main reasons of this event are intensity of depositional rate and kinetic effect that accompany to rapid degassing of CO_2 (Usdovski and Hoefs, 1990).

Both biotically induced geochemical processes such as photosynthesis and decreasing of temperature on during flow process, evaporation, mixing from soil profile or surface waters effect the variations of isotopic values (Chafetz et al., 1991b; Guo et al., 1996).

$\delta^{18}\text{O}$ ‰ PDB and SMOW with $\delta^{13}\text{C}$ ‰ PDB values of the travertine examples of Denizli basin and their bivariate distribution

Table 1- CaCO₃, δ¹⁸O and δ¹³C (PDB) values of some samples taken from Denizli travertines

Sample No	Locality	Lithofacies	CaCO ₃	δ ¹³ C‰ PDB	δ ¹⁸ O‰ PDB	δ ¹⁸ O‰ SMOW
D1	Kömürçüoğlu quarry	Shrub	100.00	0.35	-8.51	22.14
D2	Mayaş quarry	Crystalline crust	96.34	5.00	-15.10	15.34
D3	Kömürçüoğlu quarry	Shrub	100.00	0.51	-8.70	21.94
D4	Yenicekent	Crystalline crust	97.92	4.36	-13.58	16.92
D5	Kaklık Cave	Raft	96.00	1.87	-9.21	21.42
D6	Kocabaş prison	Reed	95.06	3.49	-7.95	22.71
D7	Ballık	Pisolith	99.29	2.04	-6.47	24.24
D8	Jandarma spring	Crystalline crust	94.60	6.70	-9.99	20.61
D9	Modern Travertien, Pamukkale	Crystalline crust	96.82	5.70	-11.18	19.39

show three different areas that indicate shrub+raft, pisolith+reed and crystalline crust (fig. 4).

The variations of stable isotope values in

the lithofacies deposited within the different environments (i.e. smooth and terraced slopes, shrub flats and marsh-pools of depressions) under the various conditions

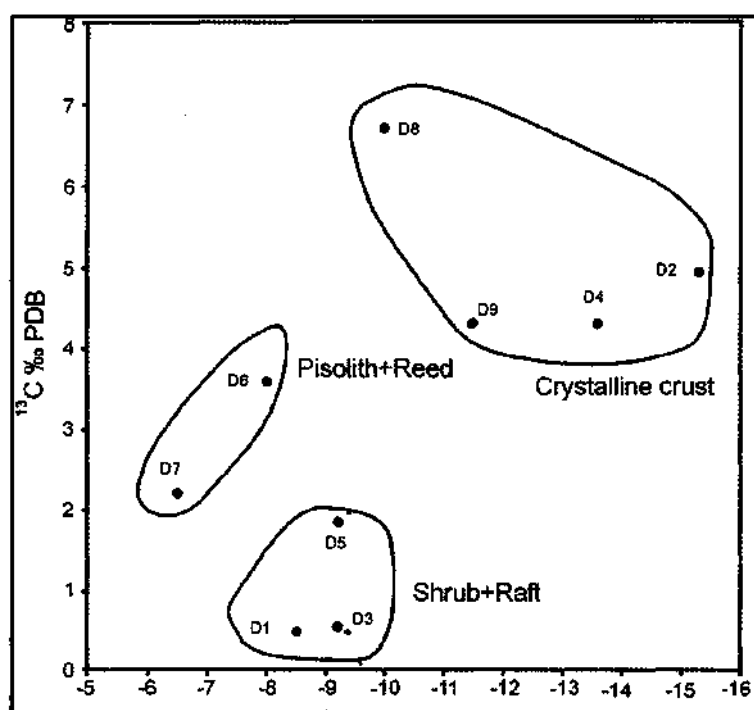


Fig. 4- Bivariate plot of δ¹⁸O ‰ SMOW and δ¹³C ‰ PDB values for the samples taken from the Denizli travertines (see Table 1).

(i.e. water temperature, flow velocity and distance from spring, surface area and biological effects) are possible. Isotopic fractionation at the thermal waters going away from the source cause a getting rich of $d^{13}C$ when removing of $d^{12}C$ together with continuously degassing of CO_2 from the thermal waters at the orifices (Chafetz et al., 1991b). Similarly, the increasing of microbiologic and photosynthetic activities in pools and depressions also result $d^{13}C$ enrichment of the system (Guo et al., 1996). All these data show that going away from the spring, travertines are enriched relatively in terms of $d^{13}C$. The same event is valid for $d^{18}O$ as well. Cooling of spring water in the flow direction and leaving of $d^{16}O$ from the system by evaporation increase $d^{18}O$ value. Linear relation of increasing of both these two isotopes in relation with distance of spring has been revealed in many studies on recent and fossil travertines (Chafetz and Lawrence, 1994; Guo et. al., 1996).

This linear relation could not be observed at the isotope values at the lithofacies representing the Denizli travertines. The $d^{13}C$ values of the shrub, raft and pisolith lithofacies, precipitated in the pools and flats away from the springs, display a distinct decrease unexpectedly (Table 1), although the expected increase of $d^{18}O$ values has been apparently realized.

CONCLUSIONS

Conclusions inferred in the study are as follows:

1- Hot water travertines of the Denizli basin have been separated into lithofacies in field scale. These are: Crystalline Crust, Shrub, Pisolith, Paper-Thin Rafts, Coated Gas Bubbles, Reed, Lithoclast, Pebbly Travertine and Paleosol Horizons. Petrographical investigations (including SEM studies) have also been made on the representative samples taken from each lithofacies.

2- The travertine lithofacies are found in different rates in the depositional environments. The crystalline crust lithofacies are seen commonly on the smooth slopes, rims of the terrace pools, vertical surfaces of the waterfall subenvironments and in extensional fissures of the travertine ridges. The light-coloured shrub lithofacies is the most common and typical component in the shrub flats of the depressions and comprises abundant diatome and bacterial filaments.

3- The dark-coloured reed travertines are particular to the reed mounds and marsh-pool subenvironments in the depressions. The reed travertines are the second order lithofacies in widespread, in related to the shrub travertines. Pisolith, Paper-Thin Raft, Coated Gas Bubble, Lithoclast and Pebbly Travertine Lithofacies are the local and restricted occurrences. The solution cavities and microkarstic features seen in a pisolith inner structure reflect more probably desiccation periods in the terrace pools where pisoliths formed.

4- The Travertines in the study area are mainly precipitated on the slope, depression, fissure ridge, mound and self-built channel environments. The slopes and the depressions are divided into smooth, terraced and shrub flat and marsh-pool subenvironments, respectively. Transitions in the vertical directions have been observed usually from the depression to slope or mound depositional environments.

5- The travertine precipitation in the depressions have been ceased by palaeosol formations, green mudstones and marl beds deposited in the marsh and shallow lakes.

6- According to the stable isotope analysis of the travertine samples, the values of $d^{13}C$ and $d^{18}O$ changes between 0.35 to 6.7 ‰ and -6.47 to -15.10 ‰, respectively. When $d^{18}O$ ‰ PDB and SMOW and $d^{13}C$ ‰ PDB values are intersected with each other, the

clumping occurrences in three different fields represent shrub+raft, pisolith+reed and crystalline crust lithofacies. Such an isotopic clumping supports that the travertines have precipitated in different depositional conditions and environments. $d^{13}C$ values are unexpectedly low in the travertine lithofacies that characterize the pools and stagnant water conditions. This statement means that the biologic induce of the $CaCO_3$ precipitation in the environment have not been enough effective enough.

ACKNOWLEDGMENTS

The fieldwork and SEM analysis of this study were supported by The Scientific and Technical Research Council of Turkey (TÜBİTAK, project no: YDABÇAG-198Y100). The authors thank to Muharrem Satır (University of Tübingen, Germany) for isotope analysis. We are grateful to Nizamettin Kazancı (Ankara University) who encouraged us to study the Denizli travertines and Robert Riding (University of Wales, Cardiff, UK) and Allan Pentecost (King's College London, UK) for some comments and literature support. During the fieldwork, the owners of Kömürcüoğlu, Mayaş, Alimoğlu, İlik, Çakmak, Emek and Ece quarries and the Kamara thermal hotel have provided logistic support.

Manuscript received November 2, 2001

REFERENCES

- Allen, E. T. and Day, A. L., 1935, Hot springs of the Yellowstone National Park: Carnegie Inst., Wash. Publ., 466, 525 pp
- Altunel, E., 1996, Pamukkale travertenlerinin morfolojik özellikleri, yaşları ve neotektonik önemler: MTA Derg., 118, 47-64.
- and Hancock, P. L., 1993a, Morphology and structural setting of Quaternary travertines at Pamukkale, Turkey: Geological Journal, 28; 335 - 346.
- and ———, 1993b, Active fissuring and faulting in Quaternary travertines at Pamukkale, western Turkey: Z. Geomorph. N. E. 285 - 302.
- Baker, G. and Frostick, A. C., 1951, Pisoliths, oololiths and calcareous growths in limestone caves at Port Campbell, Victoria, Australia: Jour. Sed. Pet., 21, 85-104.
- Bargar, K. E., 1978, Geology and thermal history of Mammoth hot springs. Yellowstone National Park, Wyoming: U.S. Geol. Surv. Bull., 1444, 55.
- Black, D. M., 1953, Aragonite rafts in Carlsbad Caverns, New Mexico: Science, 117, 84-85.
- Bozkuş, C.; Kumsar, H.; Özkul, M. and Hanger, M., 2000, Seismicity of Active Honaz fault under an extensional tectonic regime. In International Earth Science Colloquium on the Aegean Region, Dokuz Eylül Univ., Dept. of Geology, Izmir-Turkey. (Edited by O. Ö. Dora, İ. Özgenç and H. Sözbilir), Proceedings, p. 7-16.
- Canik, B., 1978, Denizli - Pamukkale sıcak su kaynaklarının sorunları: Jeoloji Mühendisliği Derg., 5, 29 -33.
- Chafetz, H. S. and Meredith, J. C. 1983, Recent travertine pisoliths (pisoliths) from southeastern Idaho, U.S.A.: In: Coated Grains, Ed. by T.M. Peryt, 450-455, Springer - Verlag, Berlin.
- and Folk, R. L., 1984, Travertines: Depositional morphology and the bacterially constructed constituents: Jour. Sedimentary Petrology, 54, 1,289-316.
- ; Rush, P. F. and Utech, N. M., 1991 a, Microenvironmental controls on mineralogy and habit of $CaCO_3$ precipitates: an example from an active travertine system: Sedimentology, 38, 107-126.
- ; Utech, N. M., and Fitzmaurice, S. P., 1991b, Differences in the $d^{18}O$ and $d^{13}C$ signatures of seasonal laminae comprising travertine stromatolites: Jour. Sedimentary Petrology, 61,6, 1015- 1028.
- and Lawrence, J.R., 1994, Stable isotopic variability within modern travertines: Geographie Physique et Quaternaire, 48, 257-273.

- Chafetz, H.S. and Guidry, S.A., 1999, Bacterial shrubs, crystal shrubs, and ray-crystal crusts: Bacterially induced vs abiotic mineral precipitation, *Sedimentary Geology*, v. 126, p. 57-74.
- Çakır, Z., 1999, Along - strike discontinuity of active normal faults and its Influence on Quaternary travertine deposition: Examples from western Turkey: *Tr. J. of Earth Sciences*, 8, 67 - 80.
- Demirkıran, Z. and Çalapkulu, R., 2001, Kaklık-Kocabaş travertenlerinin litolojik, morfolojik özellikleri ve sınıflandırılması: *Mersem 2001, Türkiye III. Mermer Sempozyumu Bildiriler kitabı*, 17-31, TMMOB Maden Müh. Odası Afyon II Temsilciliği, Afyon.
- Ekmekçi, M.; Günay, G. and Şimşek, S., 1995, Morphology of rimstone pools, Pamukkale, western Turkey: *Cave Karst Sci.*, 22, 103-106.
- Eşder, T. and Yılmaz, S., 1991, Pamukkale jeotermal kaynakları ve travertenlerin oluşumu: (Editor: N. Özer) *Tıbbi Ekoloji ve Hidroklimatoloji Dergisi*, Özel sayı
- Folk, R. L. and Chafetz, H. S., 1983, Pisoliths (pisoliths) in Quaternary travertines of Tivoli, Italy: In: *Coated Grain* (Ed. by T. M. Peryt), 474-487. Springer-Verlag, Berlin.
- ;——— and Tiezzi, P. A., 1985, Bizarre forms of depositional and diagenetic calcite in hot spring travertines, central Italy: In: *Carbonate Cements* (Ed. by N. Schneidermann and P. Harris), *Spec. Publ. S.E.P.M.*, 36, 349-369.
- Gökgöz, A., 1994, Pamukkale - Karahayıt - Gölemezli Hidrotermal Karstının Hidrojeolojisi: *Doktora tezi*, Süleyman Demirel Univ. Fen Bil. Enst. 263s., Isparta.
- and Filiz, S., 1998, Pamukkale- Karahayıt dolayındaki sıcak ve mineralli sularla travertenleri kirleten etkilerin değerlendirilmesi ve bunların önlenmesi: *Yerbilimleri (Geosound)*, 32, 29-43.
- Guo, L., 1993, *Fabrics and facies of Quaternary travertines, Rapolano Terme, central Italy*. PhD thesis, University of Wales, Cardiff, 237 pp.
- Guo, L. and Riding, R., 1994, Origin and diagenesis of Quaternary travertine shrub fabrics, Rapolano Terme, central Italy: *Sedimentology*, 41, 499-520.
- , Andrews, J., Riding, R., Dennis, P. and Dresser, Q., 1996, Possible microbial effects on stable carbon isotopes in hot-spring travertines: *Jour. Sedim. Res.*, 66, 468-473.
- and Riding, R., 1998, Hot-spring travertine facies and sequences, Late Pleistocene Rapolano Terme, Italy: *Sedimentology*, 45, 163-180.
- and ———, 1999, Rapid facies changes in Holocene fissure ridge hot spring travertines, Rapolano Terme, Italy: *Sedimentology*, 46, 1145-1158.
- Kahle, C. F., 1977, Origin of subaerial Holocene calcareous crusts: role of algae, fungi and sparmicritization: *Sedimentology*, 24, 413-435.
- Koçak, A., 1971, *Denizli-Pamukkale ve Karahayıt kaplıcalarının hidrojeolojik etüdü: MTA Rep. 5670, 21s.* (unpublished). Ankara
- Özkul, M. and Alçıçek, M. C., 2000, Facies variation in Recent to Quaternary fissure ridge hot spring travertines, Denizli Basin, Interior Western Turkey: *International Earth Science Colloquium on the Aegean Region*, Dokuz Eylül Univ. Engineering Faculty, Dept of Geology, Izmir, Turkey, Poster display, *Proceedings Abstracts*, p. 91,
- ; ———; Heybeli, H., Semiz, B. and Erten, H., 2001, Denizli sıcak su travertenlerinin depolanma özellikleri ve mermercilik açısından değerlendirilmesi: *Mersem 2001, Türkiye III. Mermer Sempozyumu Bildiriler kitabı*, 57-72, TMMOB Maden Müh. Odası Afyon II Temsilciliği, Afyon.
- Özpinar, Y. M.; Heybeli, H.; Semiz, B.; Baran, H. A. and Koçan, B., 2001, Kocabaş ve Denizli travertenlerinin jeolojik, petrografik özellikleri ve oluşumunun incelenmesi, teknik açıdan değerlendirilmesi: *Mersem 2001, Türkiye III. Mermer Sempozyumu Bildiriler kitabı*, 133-148, TMMOB Maden Müh. Odası Afyon II Temsilciliği, Afyon.

- Pentecost, A., 1990, The formation of travertine shrubs: Mammoth Hot Spring, Wyoming: Geol. Mag., 127, 159-168.
- , 1993, British travertines: A review: Proceedings of the Geologists Association, 104, 23-29.
- and Tortora, P., 1989, Bagni di Tivoli, Lazio: A modern travertine- deposition site and its associated microorganisms: Bull. Soc. Geol. Ital., 108, 315-324.
- ; Bayan, S. and Yesertener, C., 1997, Phototrophic microorganisms of the Pamukkale Travertine, Turkey: Their distribution and influence on travertine deposition: Geomicrobiology Jour., 14, 269-283.
- Srdoc, D.; Chafetz, H.S. and Utech, N., 1989, Radiocarbon dating of travertine deposits, Arbuckle Mountains, Oklahoma, Radiocarbon, 31, 619-626.
- ; Osmond, J. K., Horvatincic, N., Dabous, A., A. and Obelic, B., 1994, Radiocarbon and uranium-series dating of the Plitvice Lakes travertines, 36, 2, 203-219.
- Sun, S., 1990, Denizli Uşak arasının jeolojisi ve linyit olanakları, MTA Rep. 9985, Ankara (unpublished), Ankara
- Şentürk, R, Sayman, Y, Yalçın, H. and Ağacık, G., 1971, Pamukkale sıcak suları ve travertenleri üzerinde araştırma, DSİ. Araştırma Dairesi Başkanlığı, Ara rapor. Rapor No. Ki - 507, Ankara.
- Taner, G., 2001, Denizli bölgesi Neojen'ine ait katların stratigrafik konumlarında yeni düzenleme : 54. Türkiye Jeoloji Kurultayı Bildiri özleri, 7-10 Mayıs, Ankara, 54-79.
- Uzdovski E. and Hoefs, J., 1990, Kinetics $^{13}\text{C}/^{12}\text{C}$ and $^{18}\text{O}/^{16}\text{O}$ effects upon dissolution and outgassing of CO_2 in the system $\text{CO}_2 - \text{H}_2\text{O}$: Chemical Geology, Isotop Geoscience, 80, 109-118.
- Westaway, R., 1990, Block rotation in western Turkey. 1. Observational evidence: Journal of Geophysical Research, 95, 19857-19884.
- , 1993, Neogene evolution of the Denizli region of western Turkey: Journal of Structural Geology, 15, 37-53.

PLATES

PLATE - 1

Fig. 1 - Light-coloured, vertical crystalline crust (cc) filled in a extensional fissure. Light and dark coloured travertines on the right are deposited in the shrub flat (sf) and marsh-pool (mp) subenvironments respectively. Kocabaş village, the Fidan travertine quarry. Marker as scale =13 cm

Fig. 2 - Thin section views of white, fibrous crystalline crust (cc) developed perpendicular to depositional surface and dark micritic interlayers (m).

Fig. 3 - Thin section view of the crystalline crust. Better development of one side of the clump of the calcite crystals display a cedar tree appearance.

Fig. 4 - Light-coloured, dendritic shrub layers (s) expanding upward in the growth position and dark micritic laminae (ml). The wire-cut surface, the Ece subquarry, south of Belevi village.

Fig. 5 - Thin section views of dark and micritic shrub forms (s) expanding and branching upward in the growth position. The peripheral voids between the shrubs are filled by sparite (sp).

Fig. 6 - Pisolith travertine. Thin section views of the pisolith grains composed of smooth concentric laminae.

Fig. 7- Paper-thin raft (r) travertine laminae precipitated in the space of an extensional fissure and the lithoclasts travertine (lt) dropped down into fissure space. The Kuşgözü fissure ridge hot spring travertines, northwest of Kocabaş village.

Fig. 8 - Modern paper-thin raft (r) and coated gas bubbles (gb) formed together. The Çukurbağ hot spring, Pamukkale.

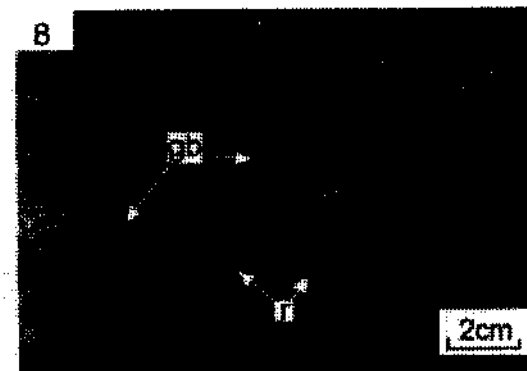
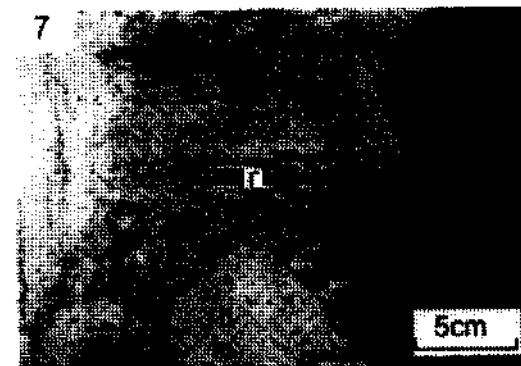
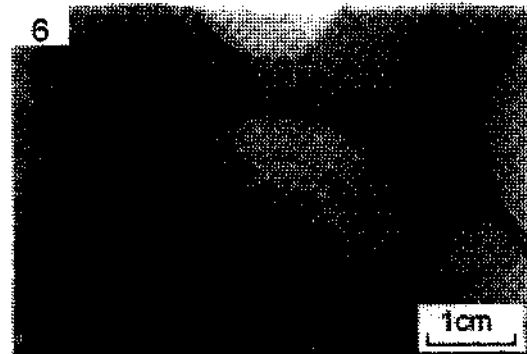
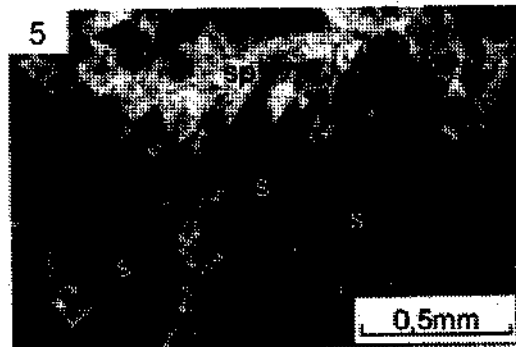
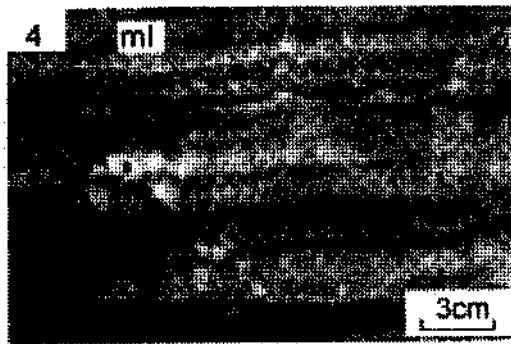
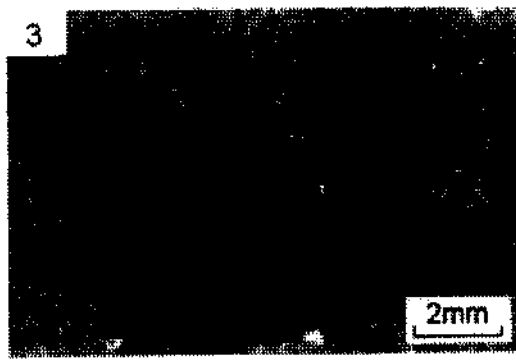
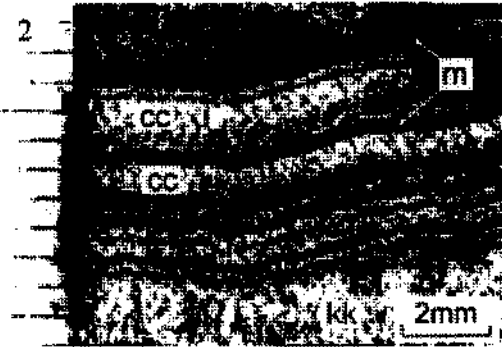
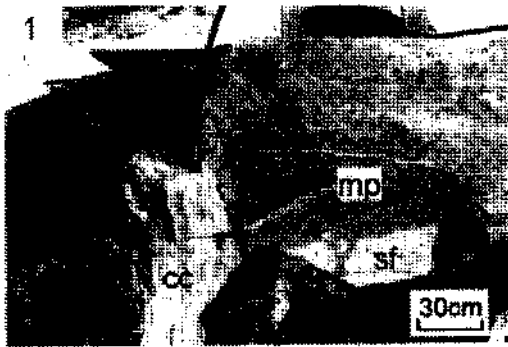


PLATE - II

Fig. 1, 2- SEM photomicrographs of smooth-edged, elongated calcite crystals (Fig. 1) and crushed crystalline crust (cc) in a micritic ground (Fig. 2).

Fig. 3- SEM photomicrographs of micrites (m) developed on the relics of spar crystals (sp), due to sparmicritization and calcified bacterial filaments (bf) at the upper left corner.

Fig. 4- SEM photomicrographs of alternation of the micrite interlayers (shown by rows) and calcite layers with radial growth in a pisolith grain. Microsolution pore (mp) on the upper right was filled by light coloured, secondary lime mud (lm).

Fig. 5, 6, 7- SEM photomicrographs of euhedral-subhedral spar crystals growing on the micritic ground. Rhombic edges of the crystals are preserved as seen in Fig. 7 or partly fractured or rounded (Fig. 6 and 7).

Fig. 8- Radial calcite crystals (cc) developed perpendicular to micritic ground (m).

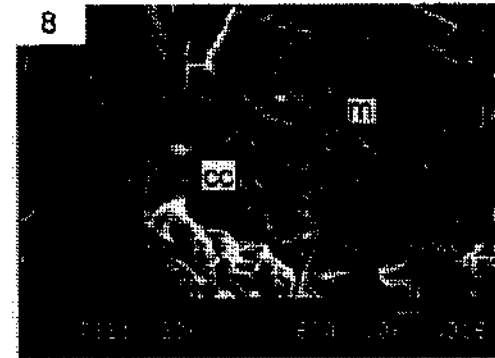
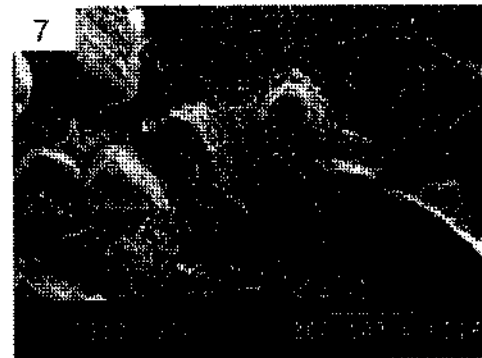
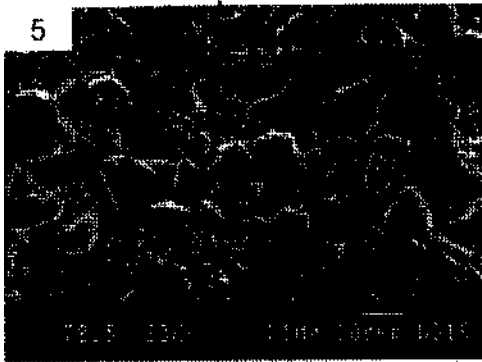
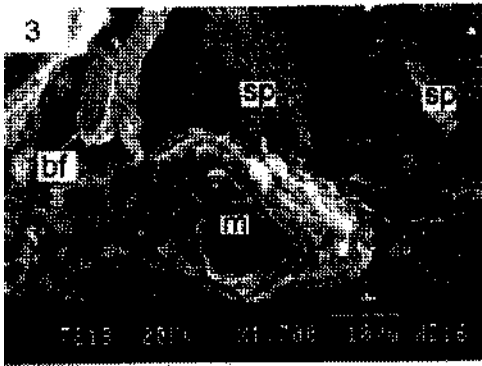
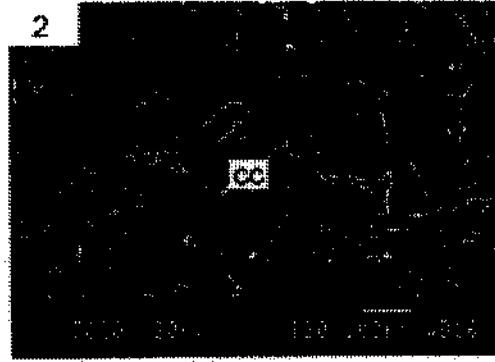
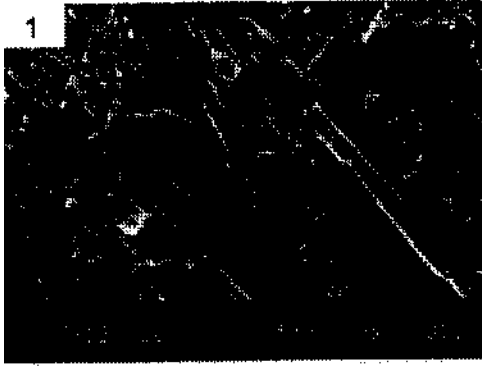


PLATE - III

Fig. 1- SEM photomicrograph of diatome relics (d) on a micritic ground of the dark coloured travertines precipitated in a marsh-pool subenvironment.

Fig. 2- SEM photomicrograph of microkarstification (mk) in internal structure of a pisolith grain and microstromatolith structure.

Fig. 3- SEM photomicrograph of close up view of a pore resulting from microkarstification between pisolith interlayers.

Fig. 4- SEM photomicrograph showing radial calcite (rc) crystals covered by thin micritic interlayers (ml) in a pisolith structure.

Fig. 5- SEM photomicrograph showing calcite crystals with radial/feathery growth in a pisolith structure.

Fig. 6- SEM photomicrograph showing the aggregate composed of ksenohedral coarser micritic grains (mg) in the nucleus of a pisolith.

Fig. 7- SEM photomicrograph showing the euhedral spar crystals as a pore fill.

Fig. 8- SEM photomicrograph showing probably bacteria-induced structure in the micritic levels of the travertines.

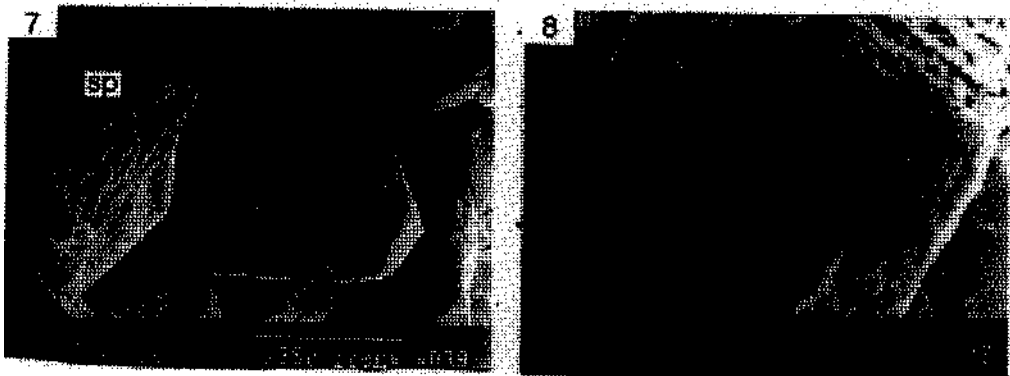
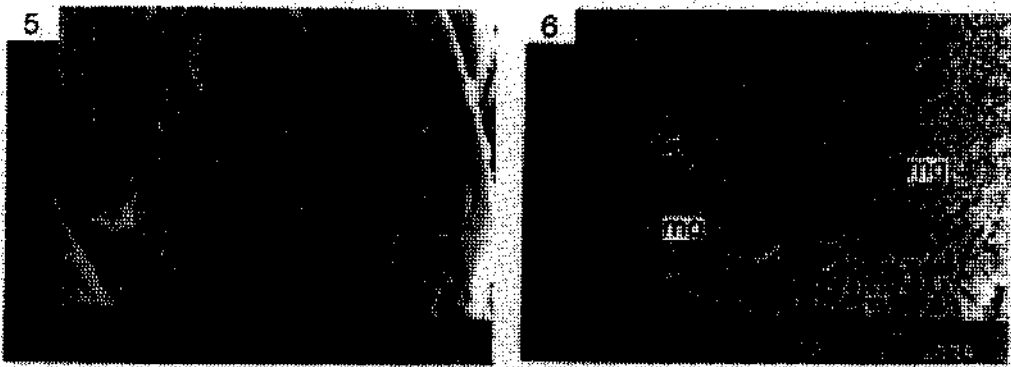
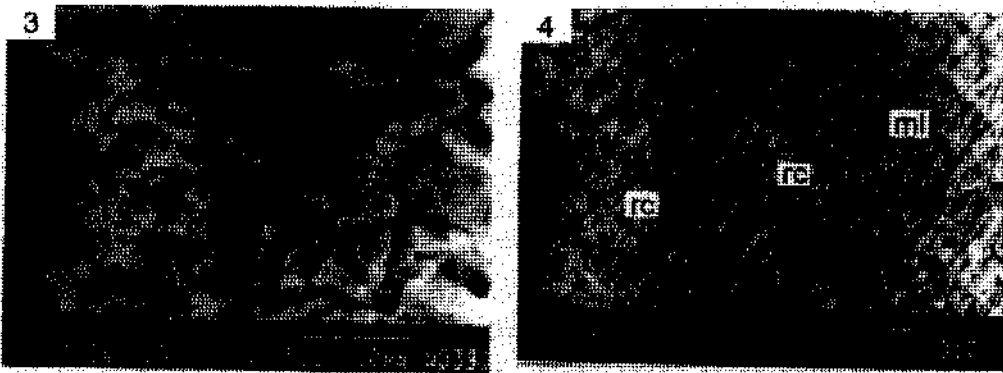
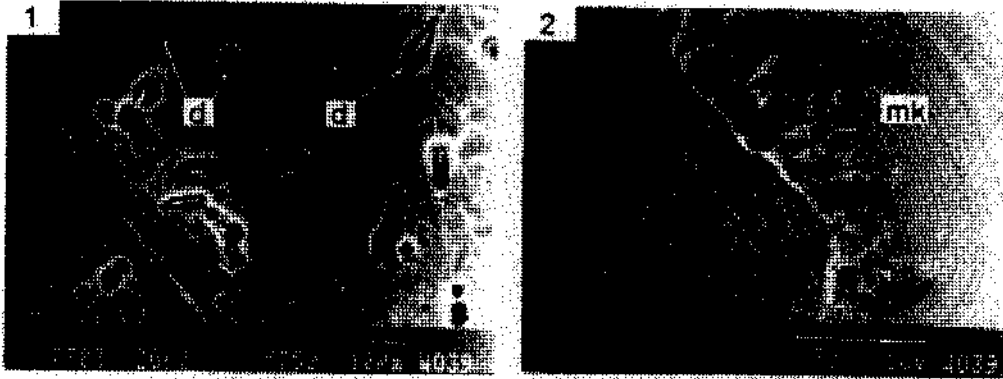


PLATE - IV

Fig. 1- Smooth and terraced slope subenvironments of a slope depositional environment at recent Pamukkale travertines. ss= smooth slope, ts= terraced slope.

Fig. 2- Microterrace pools developing on a vertical wall. The Kırmızısu hot spring, Karahayıt, Scale: Marker=13 cm.

Fig. 3- Vertical travertines deposited a waterfall subenvironment resembling an overhanged curtain (ohc) and composed of mainly crystalline crust lithofacies, The northern slope of Keltepe, near Dereköy village.

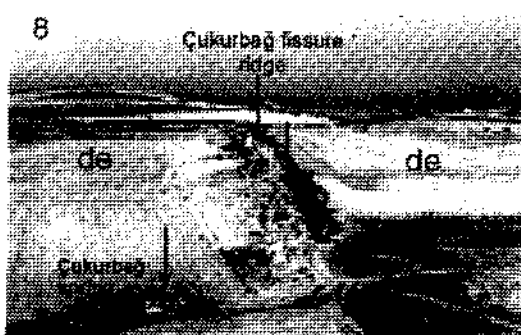
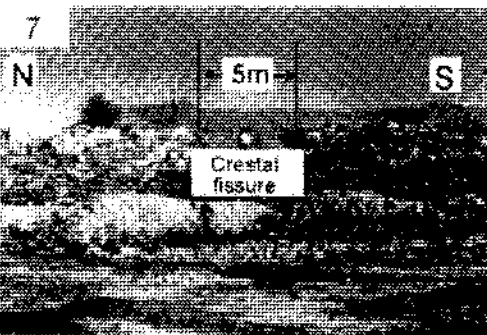
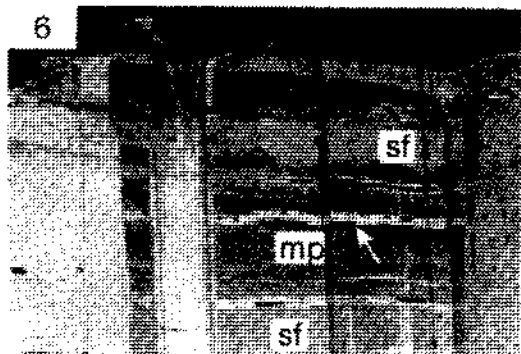
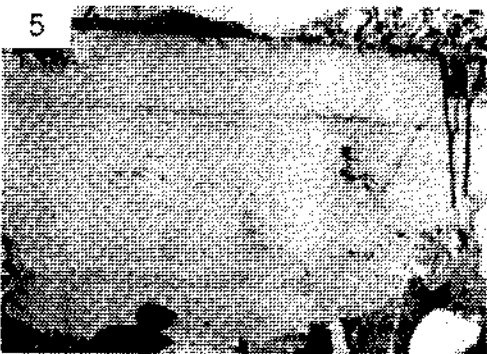
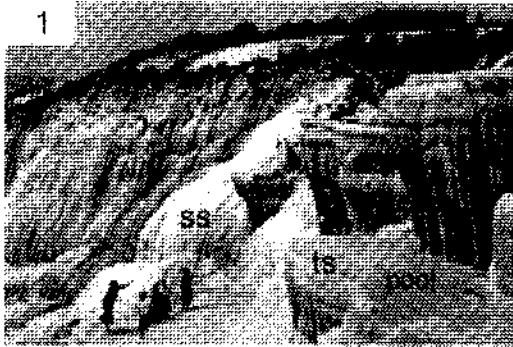
Fig. 4- General view of bedded travertines deposited in shrub and marsh-pool subenvironments of depressional fields. Emek quarry, Kocadüz locality, northwest of the Denizli Cement Factory.

Fig. 5- Horizontal bedded, light coloured travertine deposited a shrub subenvironment, wire-cut surface, the İlik quarry, southern slope of Killiktepe, northwest of Kaklık.

Fig. 6- Horizontal, light coloured shrub flat (sf) and dark coloured marsh-pool (mp) travertines deposited in the depressional field neighbouring a fissure ridge and stratified layers of white crystalline crust lithofacies (arrowed).

Fig. 7- The view of the Kuşgölü fissure ridge from the west. E-W trending main fissure at the west part of the ridge is 5 m in thickness.

Fig. 8- North-west trending the Çukurbağ fissure ridge (arrowed in the middle) and adjacent depressional deposition environments (de) with low topography lying on the each sides of the ridge. The Çukurbağ thermal spring located at the southern end of the ridge (arrowed in the lower left), Pamukkale.



MOLLUSCAN FAUNA AND STRATIGRAPHY OF THE UÇARSU AND KASABA FORMATIONS AT KASABA MIOCENE BASIN (WESTERN TAURIDES, SW TURKEY)

Yeşim İSLAMOĞLU* and Güler TANER**

ABSTRACT.- In the study, six stratigraphical section has been measured through mollusc-rich Uçarsu and Kasaba formations, outcropping at Kasaba Miocene Basin in western Taurides. By evaluating the paleogeographic and chronostratigraphic denotations of mollusc species, it has been concluded that, most of the samples were Mediterranean Tethyan in origin and the other forms, such as *Divaricella ornata subornata* Hilber, *Cerithium zejsneri* Pusch and *Pitar (Paradione) lilacinooides* Schaffer, that were peculiar to the central Paratethys have also been determined. So, for the investigation area, the Paratethyan marine stages were pictured too. By these findings, the age of the shallow-marine Uçarsu formation has been inferred as Upper Burdigalian (Upper Eggenburgian-Carpathian) and that of the other shallow-marine Kasaba formation as Langhian (Lower Badenian). The former is transgressive in nature at its basal parts and characteristically regressive toward the top, while the latter, grading into continental environment from a steady shallow marine, displays regressive character throughout. By context of the paleontological data from Uçarsu and Kasaba formations and superposing of the (studied) units, it is suggested that the emplacement of the Yeşilbarak nappe and the Lycian nappes into the region had initiated in the Upper Burdigalian and continued until the end of the Langhian.

INTRODUCTION

Kasaba Miocene Basin lies at the western side of gulf of Antalya, on the Teke peninsula, between Elmalı and Kaş townships (Fig. 1). Within the investigation area, the Miocene-aged units are observed within the Beydağları Autochton and Yeşilbarak nappe.

In the course of study, just two amongst the mollusc-bearing Miocene-aged units, the Uçarsu and Kasaba formations has been looked at thoroughly, and four sections from the former and two on the latter were traversed (Fig. 1). Along these, totally sixty-nine taxons have been recognized (İslamoğlu, 2001) and by examining the paleogeographic and chronostratigraphic denotations of those, ages of the formations could have been inferred (Table 1).

GEOLOGY

Initial works at the region were carried out by Lucius (1925), Kirk (1932), Mankiewicz (1946), Colin (1955), Holzer (1955), Flugel (1961) and Pisoni (1967).

The units at the region were subdivided into Beydağları autochton, Lycian nappes and Yeşilbarak nappe (Şenel, 1997a,b,c), and one of which, the Beydağları autochton has been subjected to detailed studies by several researchers (Colin, 1962; Poisson, 1977; Önalın, 1979; Erakman et al., 1982; Yalçınkaya et al., 1986; Şenel et al., 1989, 1994). The lowermost portion of the autochton is Jurassic-Upper Cretaceous-aged Beydağları formation, that extends over large areas and deposited at carbonate shelf environment, including patch reefs composed of rudists at its basal part (Şenel et al., 1989,

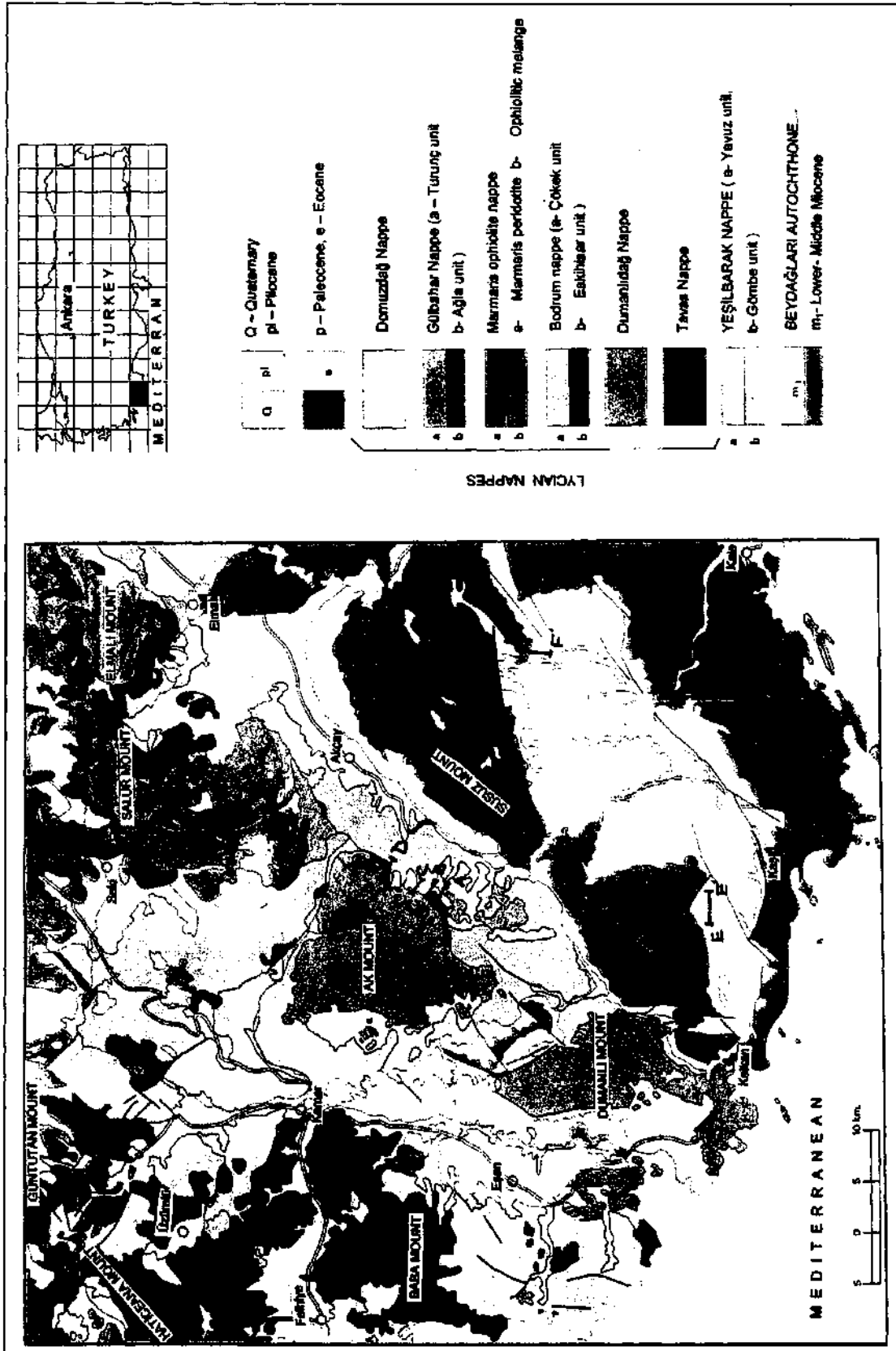


Fig. 1 - Geological map of the Kasaba Miocene basin and surrounding area (adapted from Şenel, 1997 a,b,c). AA'- Bozgediktepe section, BB'- Akçaşapınarı section, CC' Uçarsu section, DD'- Sıradona section, EE'- Boyacıpınarı section, FF'- Ortabağ section.

1994). Covering that unit, the Gedikbaşı formation, neritic limestone in nature, accumulated during Paleocene and sits on probably unconformably (Önalın, 1979; Şenel et al., 1989, 1994). Resting unconformably upon the Gedikbaşı formation, the Susuzdağı formation represents Upper Lutetian-Priabonian age and settled down at shallow carbonate shelf fades (Önalın, 1979; Şenel et al., 1989, 1994). The following units are transgressive Karabayır formation, Aquitanian in age and Burdigalian-aged Sinekçi formation, respectively. Sinekçi formation is also transgressive and has been subdivided into three members, Gümüce algal limestone, Kıbrısdere clayey limestone and Çayboğazı claystone by Önalın (1979). Kasaba formation, sedimented during Langhian (Lower Badenian) overlies that unit. Both Kasaba and Sinekçi formations are tectonically capped by Elmalı formation, which is a component of Gömbe group in Yeşilbarak nappe (Şenel et al., 1989, 1994). The uppermost unit extending in the region is Felenkdağ conglomerate, blanketing the Miocene-aged units unconformably.

Lycian nappes have previously been called as Elmalı nappes and Lycian nappes by Colin (1962), Brunn et al. (1971), Önalın (1979), Erakman et al. (1982), Günay et al. (1982), Bölükbaşı (1987) and that has been subdivided into Tavas nappe, Bodrum nappe, Dumanlıdağ nappe, Marmaris ophiolitic nappe, Gülbahar nappe and Domuzdağ nappe by Şenel et al. (1987, 1989, 1994) and Şenel (1997a,b,c).

Another tectonic unit, seen in the region is Yeşilbarak nappe. Resting at the base of the nappes, that unit displays a lateral continuity between the autochton and the nappes (Önalın, 1979; Şenel et al., 1986, 1987, 1989, 1994 and Şenel 1997a,b,c) (Fig. 1).

the unit has been separated into two sub-structural units, the Gömbe group and Yavuz formation by Şenel et al. (1989), and of which, just one, the Gömbe group can be seen through investigation area. Gebeler formation, characterizing the base of the Gömbe group, deposited during Cenomanian-Santonian (Upper Cretaceous), outcrops outside the area. The overlying unit, transgressive Elmalı formation is composed entirely of turbiditic elastics, representing a Upper Lutetian-Lower Miocene age (Önalın, 1979). That formation appears around Gömbe and Elmalı.

The area and the surrounding region had undergone the compression regime, caused by the Alpine orogeny (Colin, 1962; Brunn et al., 1971; Özer et al., 1974; Poisson, 1977; Önalın, 1979; Erakman et al., 1982; Akay et al., 1985; Şenel et al., 1987, 1989, 1994; Robertson, 1993; Şenel, and Bölükbaşı, 1997. Antalya nappes had initially moved from east-northeast during Senonian and consequently, during Danian they placed on the eastern and northeastern flanks of the autochton. Later on, these nappes had been pushed onto the Beydağları autochton, in east-west direction (Şenel et al., 1992, 1994). Lycian nappes, had probably clustered at the north of Menderes massif by the closure of Cretaceous, lodged in the south at the end of Eocene. All these allochthonous units, overriding the Yeşilbarak nappe, fell into the northern and western sides of the autochton during Miocene period (Şenel et al., 1992, 1994) and that movement produced considerable effects on the Lower-Middle Miocene-aged sediments. As a consequence of oppositely thrustings, a huge amount of the elastics was transported into the basin, and that material formed the alluvial fans and fan deltas on the

coastal zone and the submarine fans in the basin, as a result of deposition. During tectonically steady-state phases, the small-scale patch reefs accumulated over the fan deltas (Hayward, 1982, 1984; Hayward and Robertson, 1996). Depending upon the extension regime following the emplacement of the nappes, Upper Miocene-Pliocene aged grabens developed (Şenel, 1997a,b,c).

LOCATIONS OF THE MEASURED SECTIONS

Bozgediktepe section (AA'). - This section lies in Fethiye O23-d₄ quadrangle and has been measured at almost 400 m northwest of Bozgediktepe. Extending southeast to northwest, it is introduced at X₁: 33750, Y₁: 44350 and that terminates at X₂: 33630, Y₂: 44600 intersects. That has been crossed in Uçarsu formation and ranges 92 m, of which the basal 52 m is represented by sandstone-mudstone, and the following 40 m by polygenie conglomerates (Fig. 2).

Akçasupınarı section (BB'). - That section, in the Fethiye O23-d₄ sheet, has been traversed in east-west direction at some 1.5 km northeast of Yaskam locality. It begins at X₁: 34350, Y₁: 47075 intersect and comes up to an end at X₂: 34650, Y₂: 47100. Reaching up a thickness approximately 225 m, that also characterizes part of Uçarsu formation (Fig. 3).

Uçarsu section (CC'). - Depicted from Uçarsu spring in Fethiye O23-d₄ rectangle, that section ranges from X₁: 34375, Y₁: 48380 to X₂: 34250, Y₂: 48600 points and of which thickness reaches to 66 m. That also represents a portion of Uçarsu formation (Fig. 4).

Sıradona section (DD'). - That section has been picked up at some 850 m northwest of Çukurbağ, in Fethiye O23-d₃ quadrilateral,

through a northeast-southwest direction. Stretching for 137 m, it has been introduced at X₁: 36130, Y₁: 49580 intersect and of which termination is at X₂: 35900, Y₂: 49500 point (Fig. 5).

Boyacıpınar section (EE'). - Going over Fethiye P23-a₄ sheet, this section has been practiced between X₁: 31750, Y₁: 18800 and X₂: 32750, Y₂: 18400 points, at nearly 950 m southwest of Boyacıpınar. Given a thickness reaching 67 m in Kasaba formation, it stretches toward south firstly and then turns up to southwest (Fig. 6).

Ortabağ section (FF'). - That section extends in Fethiye P23-b₂ quadrangle, between X₁: 49800, Y₁: 32740 and X₂: 49820, Y₂: 32500 intersects. It has been examined in a north-south direction at 3 km south of Ortabağ and is 18 m thick (Fig. 7).

STRATIGRAPHY

Uçarsu formation, one of molluscs-bearing Miocene units, is included in Gömbe group, a member of Yeşilbarak nappe and overlies the Elmalı formation while the other one, Kasaba formation is in Beydağları autochton and covers Sinekçi formation. Generalized stratigraphic columns of both the autochton and Gömbe group are displayed in Figs. 8 and 9.

Uçarsu formation

Description. - Although Önalın (1979) has observed the unit, consisting of light-brown colored limestones around Uçarsu and Akçasupınarı and has thought that as a part of Çayboğazı member, included in Sinekçi formation, Şenel et al. (1989) has called it as Uçarsu formation, since it has appeared in a different structural unit.

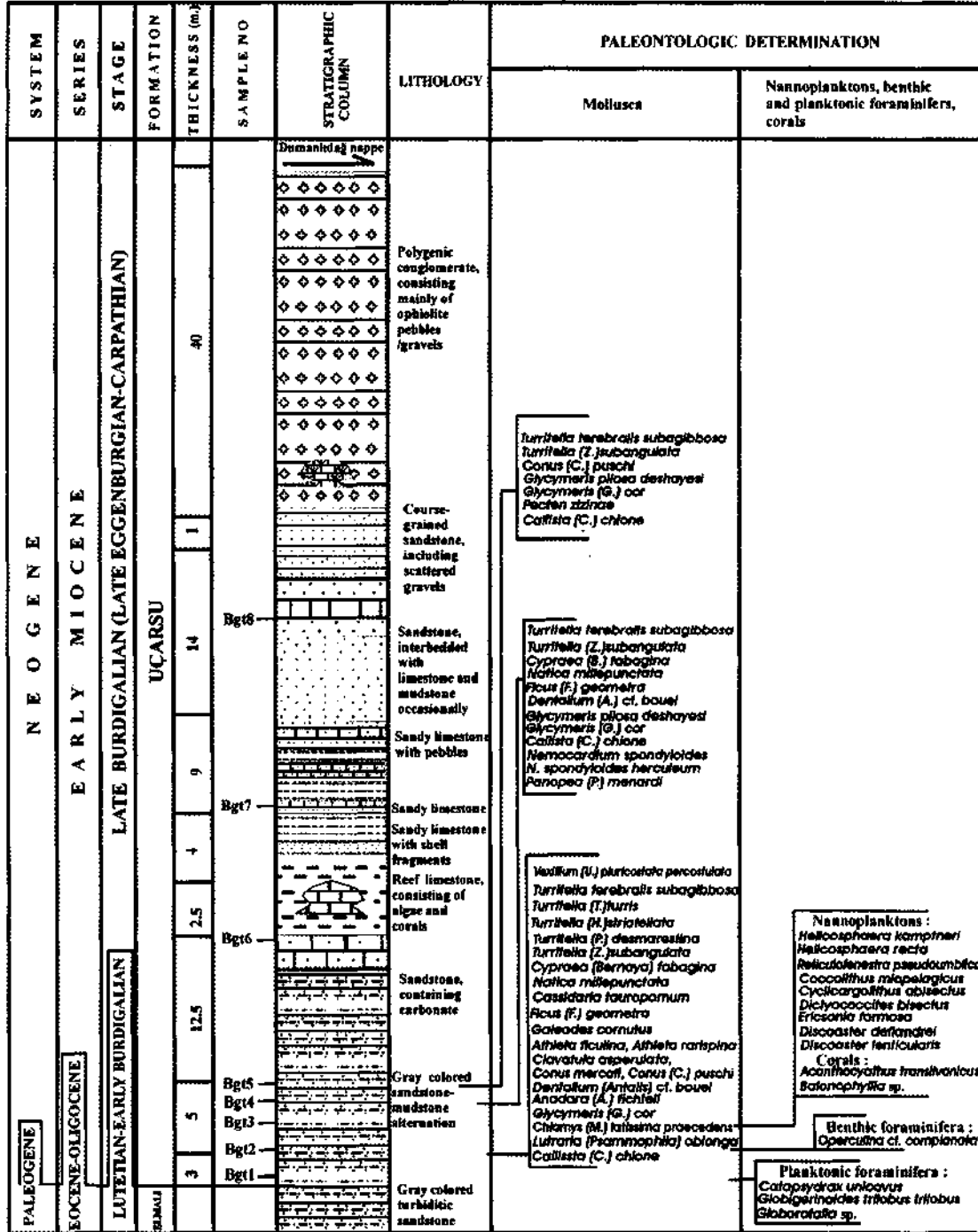


Fig. 2- Bozgediktepe stratigraphic section

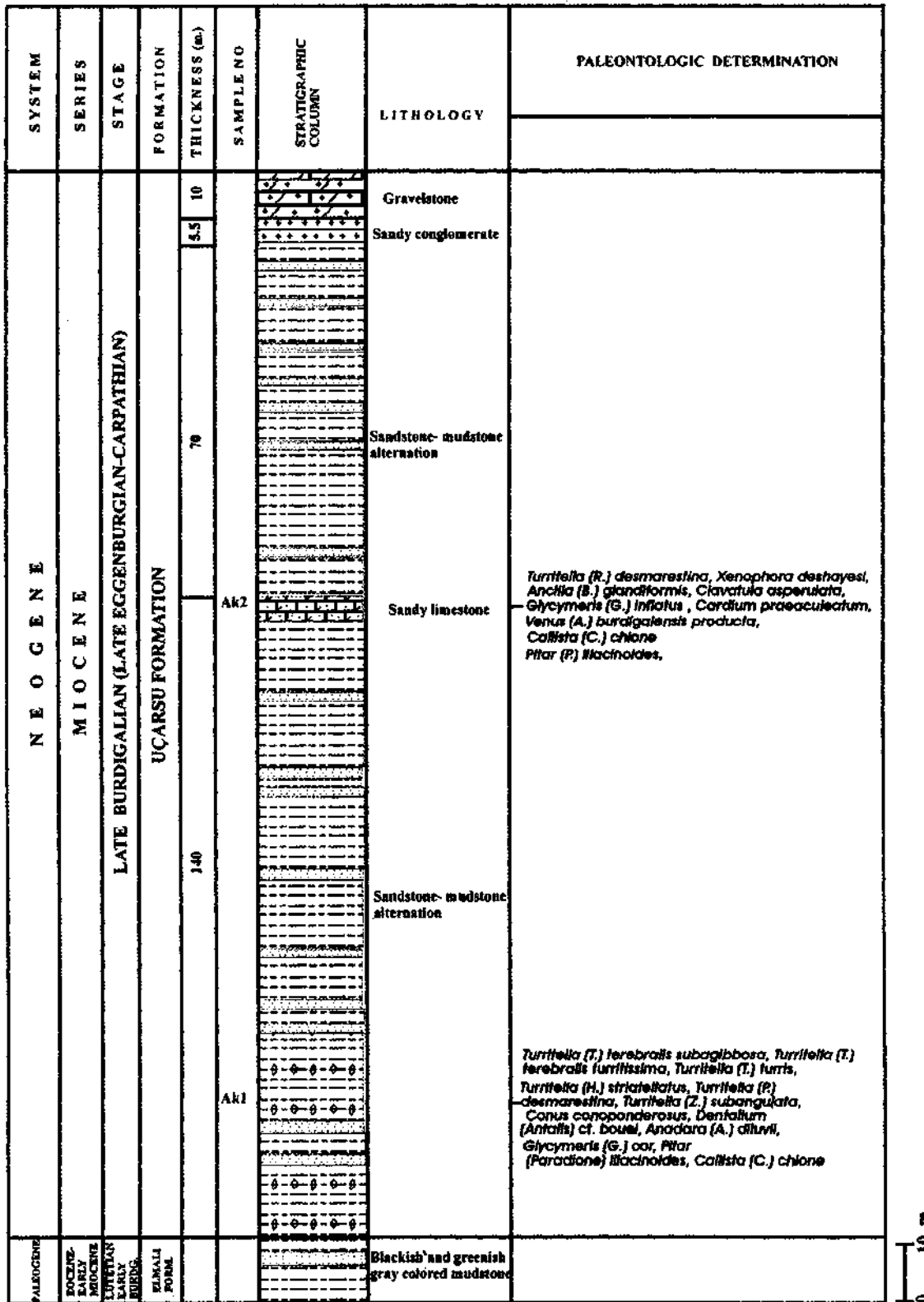


Fig. 3- Akçasupınarı stratigraphic section

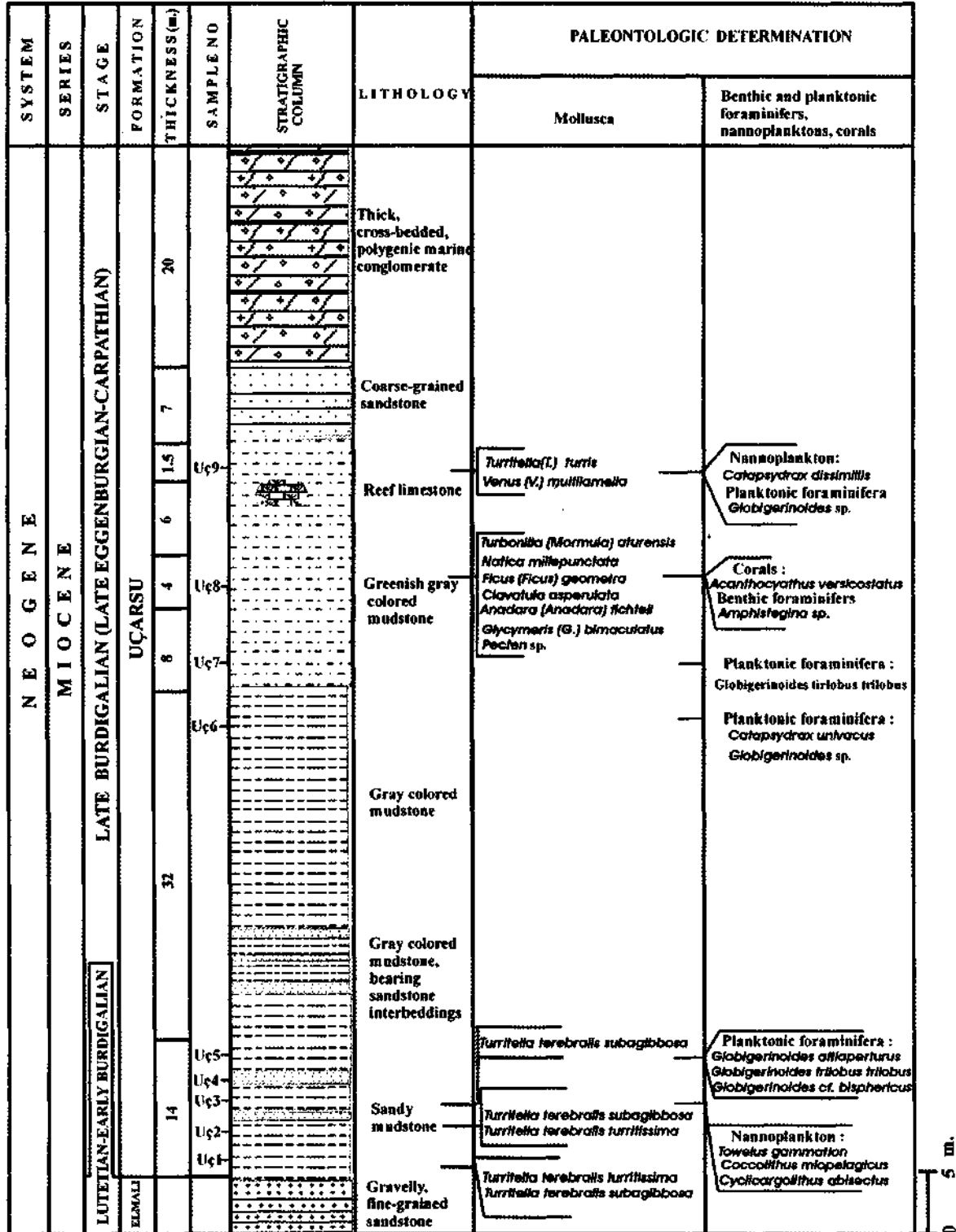


Fig. 4- Uçarsu stratigraphic section

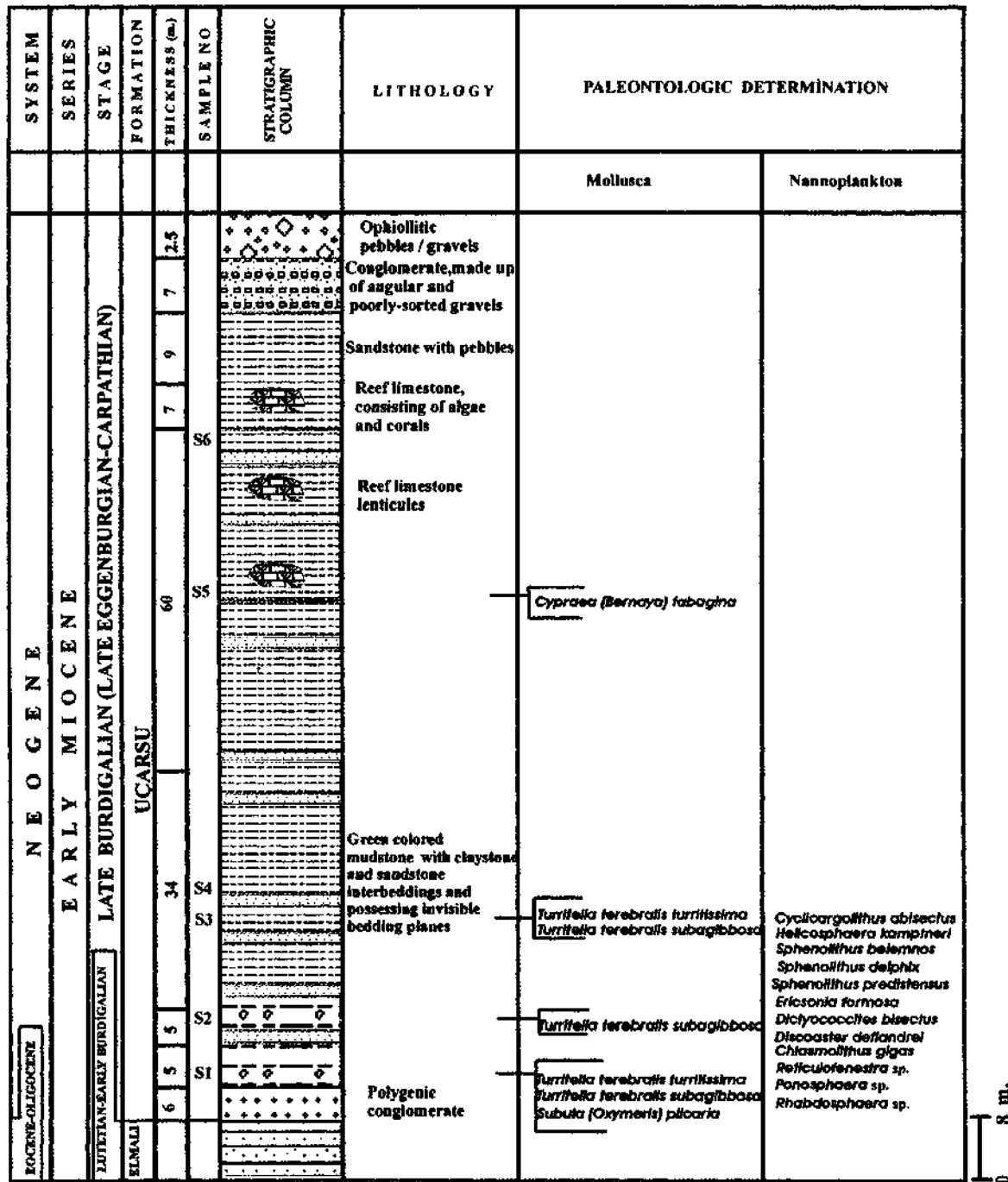


Fig. 5- Sradona stratigraphic section

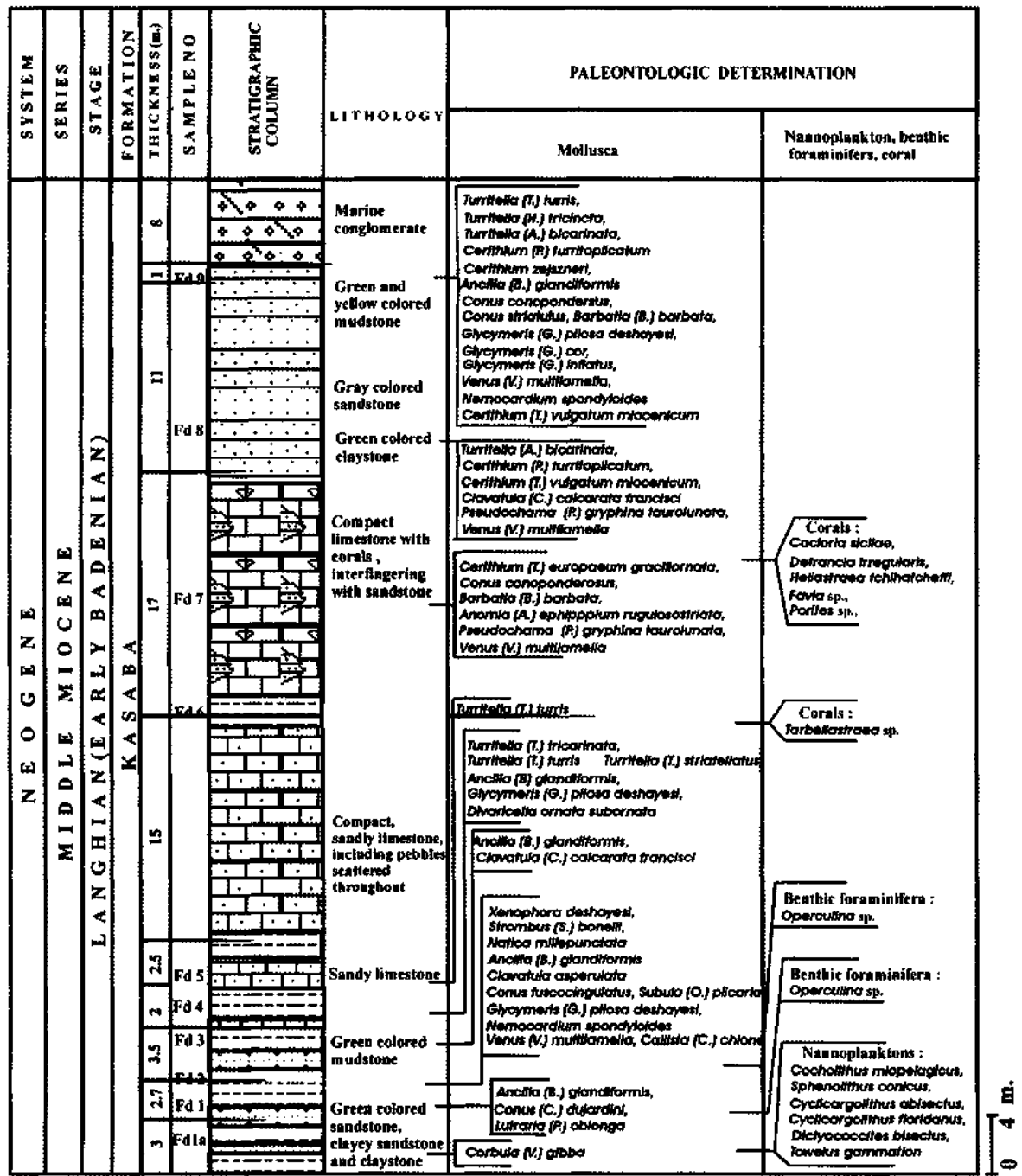


Fig. 6- Boyacıpinar stratigraphic section

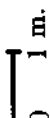
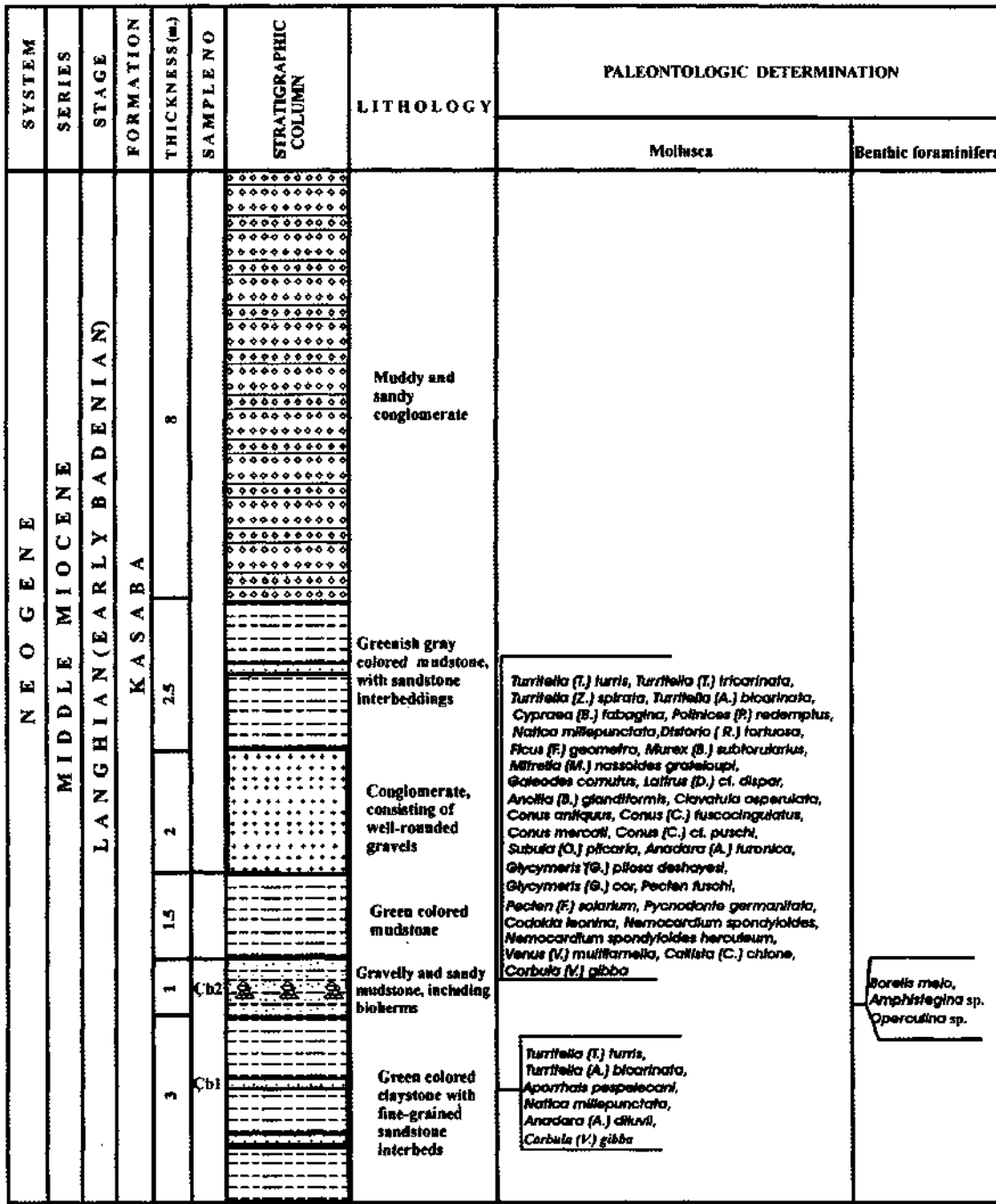


Fig. 7- Ortobağ stratigraphic section


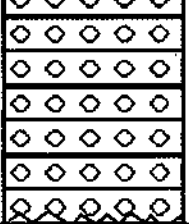
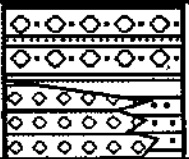
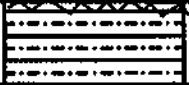


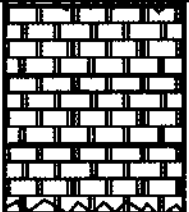
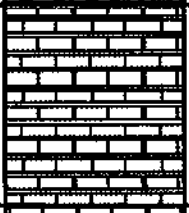
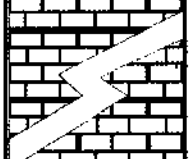
ERA (THEM)	PERIOD (SYSTEM)	SERIES (EPOCH)	STAGE	SUB-STAGE	FORMATION	MEMBER	THICKNESS (m)	LITHOLOGY			
								SECTION	EXPLANATION		
CENOZOIC	TERTIARY	NEOGENE	QUATERNARY						Loose and cemented slope-wash; alluvium and beach sands ANGULAR UNCONFORMITY		
										Conglomerate, made up of angular and rounded limestone pebbles-gravels; bearing red-colored mudstone lenticules and interbeddings UNCONFORMITY	
						SERRAVALLIAN ?		FELENİKDAĞ CONGLOMERATE	250		
					MIOCENE	LANGHIAN EARLY BADENIAN		KASABA	0-400		Thick-bedded conglomerate; fine-medium-thick bedded sandstone, siltstone, mudstone; containing few reef limestone lenticules UNCONFORMITY
						BURDIGALIAN	LATE	SİNEKÇİ	70-450		Fine to medium layered, gray to greenish gray colored, and fine-medium-thick calcarenite interbedded claystone
						EARLY		GÖMÜÇE	0-10		Fine-to medium bedded clayey limestone
									20-200		Medium- to thick layered algal limestone (BAUXITE) ANGULAR UNCONFORMITY
					PALEOGENE			SUSUZDAĞ	370		UNCONFORMITY
					EOCENE	UPPER LUTETIAN- PRIABONIAN		GEDİKBAŞI	70		Neritic limestone; medium- to thick layered; cream and light brown in color
					PALEOCENE						
					UPPER SENONIAN	Coniacian- Maestrichtian		BEYDAĞLARI	600		Medium- to thick bedded, light cream, cream, grayish white and/or light brown colored neritic limestone; infrequent dolomitization usually at rudist patch reefs

Fig. 8- Beydağları stratigraphic column of the Beydağları autochthon (after Şenel et al, 1994)

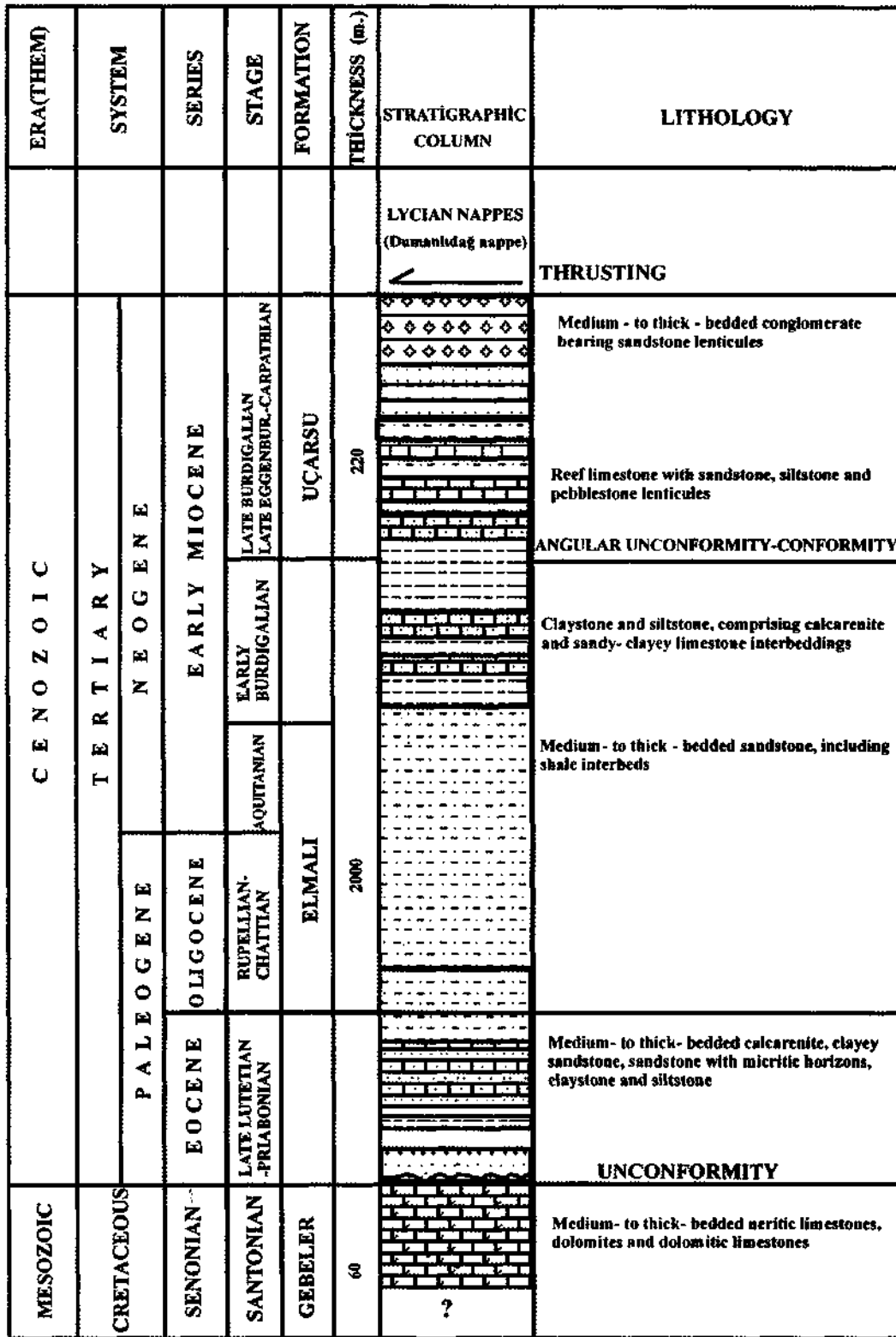


Fig. 9- Generalized stratigraphic section of Gömbe group (after Şenel et al, 1994)

Type locality. - Uçarsu spring.

Localities of the sections. - Akçasupınarı, Siradona locality, Bozgediktepe and southern and southeastern flanks of Akçağ.

Contact relationships. - Uçarsu formation sits on Elmalı formation with angular unconformity through Uçarsu and Siradona sections while covers it conformably at ones, so-called Bozgediktepe and Akçasupınarı. The formation is underlain tectonically by Dumanlıdağ nappe, the lowermost slab of Lycian nappes.

Lithology. - Uçarsu formation consists up of light-dark gray and greenish gray colored conglomerate, sandstone, mudstone and reef limestones occasionally. The lower parts are predominated by macrofossil-rich sandstone and mudstone whilst the upper levels are characterized by polygenic conglomerate.

At the base of Bozgediktepe section, gray colored and unstratified mudstone (Uçarsu formation) overlies conformably the gray colored sandstone of Elmalı formation (Fig. 2). Along the first 20 m of the section, a medium-layered, gray colored sandstone and mudstone alternates with each other. Then, sandstone grades into sandy limestone by increase in carbonate content and that sandstone and sandy limestone interval reaches up to 15 m. On that, a sandstone including scattered gravels sits and the uppermost sect is made up of polygenic conglomerate including poorly sorted and angular limestone and ophiolite pebbles. Dumanlıdağ nappe overlies that sect tectonically. Through the section, fining upward in grain size, presence of intervening reef limestones consisting of algae and coral and then grain size coarsening again imply that the sequence was transgressive at first and then regressive.

Akçasupınarı section is predominated by an alternance of thin-medium layered and greenish gray colored mudstone with thin layered, calcareous sandstone interbeddings (Fig. 3), stretching for approximately 200 m. Then, a 5.5 m thick sandy pebblestone and conglomerate, reaching up to 10 m, blanket that level, respectively.

Uçarsu section initiates with poorly-stratified and greenish gray colored sandy mudstone, including poorly-sorted and weakly-rounded pebbles (Fig. 4). That level is 70 cm thick. The next interval is a greenish gray colored sandstone and mudstone alternation, reaching to 4.5 m in thickness. That sequence goes on with the brown colored sandstone (1 m) and gray colored mudstone. The mudstone encloses limestone lenticules, involving algae and corals, in its upper part. Further on, coarse grained sandstone and the terminating deposit, polygenic conglomerate have been penetrated.

The basal part of Syradona section exhibits a polygenic conglomerate, embracing angular, moderately to well-cemented, poorly sorted, graded pebbles-gravels and finer elastics (Fig. 5). Measuring 6 m, that horizon is overlain by a greenish gray-green colored, medium-layered pebblestone-sandstone-mudstone alternation. The latter reaches to 5 m. The superimposing is the green colored mudstone, spreading out 5 m. The lower parts of the section is Gastropoda and nannoplankton-rich, although the upper parts enclose 3 to 4 m thick reef limestone lenticules, made up of algae and corals. The further one is the 8 m thick, poorly sorted and gray-brown colored gravelly sandstone. The 7 m thick polygenic conglomerate, comprising angular and poorly-sorted pebbles-gravels is the successive rock-type. At top of that succession, large

olistostromes, reaching 2.5 m and including ophiolite pebbles-gravels are seen.

Thickness.- The formation displays a thickness, reaching 225 m.

Fossil content and age.- The formation contains Upper Burdigalian (Upper Eggenburgian-Carpathian)-aged mollusc assemblage (Table 1). Especially, *Cassidaria tauropomum* (Sacco), *Vexillum (Uromitra) pluricostata percostulata* (Sacco), *Pecten zizinae* Blanckenhorn, *Chlamys (Macrochlamys) latissima praecedens* (Sacco), *Pitar (Paradione) lilacinoides* (Schaffer), *Cardium praeculeatum* Hölz and *Venus (Antigona) burdigalensis producta* Schaffer are the species that had disappeared at the end of Lower Miocene. *Turritella terebralis turritissima* Sacco and *Turritella (Peyrotia) desmarestina* Basterot are the species, that have been found only in Upper Burdigalian so far. Meanwhile, the species *Pitar (Paradione) lilacinoides* (Schaffer), *Cardium praeculeatum* Hölz and *Venus (Antigona) burdigalensis producta* Schaffer have only been found in Eggenburgian stage of central Paratethys. It is also known that, several species are introduced in marine stages of central Paratethys too, namely Eggenburgian, Ottangian and Carpathian. Therefore, referring to both names for those stages has been preferred.

The ages hold by the planktonic foraminifera and nannoplanktons support the suggested periods for the formation. The following lines will explain the determined fossils and the intervals that they have been contained in, through the sections.

a) Bozgediktepe section departs with gray colored, unstratified mudstone (Fig. 2). In that level the planktonic foraminifera, *Catapsydrax unicavus* Bolli, Loeblich and Tap-

pan, *Globigerinoides trilobus trilobus* (Reus) and *Globorotalia* sp., implying Burdigalian period were determined (Sample Bgt-1, determination by Hakyemez, A.). The overlying gray colored sandstone, from which Sample Bgt-2 was taken, embraces molluscs at high quantities. Gastropoda, *Turritella terebralis turritissima* Sacco, *Turritella (Turritella) turris* Basterot, *Turritella (Haustator) striatellatus* Sacco, *Turritella (Zaria) subangulata* (Brocchi), *Turritella (Peyrotia) desmarestina* Basterot, *Cypraea (Bernaya) fabagina* Lamarck, *Natica millepunctata* Lamarck, *Cassidaria tauropomum* (Sacco), *Ficus (Ficus) geometra* (Borson), *Galeodes cornutus* (Agassiz), *Vexillum (Uromitra) pluricostata percostulata* (Sacco), *Athleta ficulina* (Lamarck), *Athleta (Athleta) rarispina* (Lamarck), *Clavatula asperulata* (Lamarck), *Conus mercati* Brocchi, *Conus (Chelyconus) puschi* Michelotti, *Conus (Conolithus) dujardini* Deshayes, scaphopods, *Dentalium (Antalis) cf. bouei* Deshayes and Bivalvia, *Anadara (Anadara) fichteli* (Deshayes), *Glycymeris (Glycymeris) cor* (Lamarck) *Chlamys (Macrochlamys) latissima praecedens* (Sacco), *Lutraria (Psammophila) oblonga* Chemnitz, *Callista (Callista) chione* (Linne) and benthic foraminifera, *Operculina cf. complanata* DeFrance (representing usually Miocene period) have been sampled (determination by Sirel, E.).

Within that level, from which Sample Bgt-3 has been collected, a nannoplankton fauna, exemplified by *Helicosphaera kamtneri* Hay-Mohler, *Helicosphaera recta* Haq, *Reticulofenestra pseudoublica* (Gartner), *Sphenolithus conicus* Bukry, *Coccolithus miopelagicus* Bukry, *Cyclicargolithus abisectus* (Muller), *Dictyococcites bisectus* (Hay-Mohler-Wade), *Ericsonia formosa* (Kamptner), *Discoaster deflandrei* Bramlette-Riedel, *Discoaster*

lenticularis Bramlette-Sullivan characterizes late Lower Miocene-earliest Middle Miocene time interval (determined by Karakullukçu, H.). Besides those, a species belonging to ahermatype corals, living in beneath the photic zone of open shelf and characterizing the deeply waters, *Acanthocyathus transilvanicus* (Reuss), *Balonophyllia* sp. was held in (determined by Babayiğit, S.). That finding stresses that, until that level the environment has increasingly deepen.

The following 30 cm thick, gray colored sandstone is also productive for different species of Mollusca, illustrated by Gastropoda, *Turritella terebralis subagibbosa* Sacco, *Turritella (Zaria) subangulata* (Brocchi), *Cypraea (Bernaya) fabagina* Lamarck, *Natica millepunctata* Lamarck, *Ficus (Ficus) geometra* (Borson), Scaphopoda, *Dentalium (Antalis) cf. bouei* Deshayes, *Dentalium* sp. and Bivalvia, *Glycymeris pilosa deshayesi* (Mayer), *Glycymeris (Glycymeris) cor* (Lamarck), *Callista (Callista) chione* (Linne), *Nemocardium spondyloides* (Hauer), *Nemocardium spondyloides herculeum* Dollfus-Cotter-Gomez, *Panopea (Panopea) menardi* (Deshayes) (Fig. 2, Sample Bgt-4). Amongst the covering package, consisting of 1 m thick mudstone, 40 cm thick sandstone and again 1 m thick mudstone, from bottom to top, has only the last been exemplified by Sample Bgt-5, and that has been disclosed to include Gastropoda, *Turritella terebralis subagibbosa* Sacco, *Turritella (Zaria) subangulata* (Brocchi) and *Conus (Chelyconus) puschi* Michelotti and Bivalvia, *Glycymeris pilosa deshayesi* (Mayer), *Glycymeris (Glycymeris) cor* (Lamarck), *Pecten zizinae* Blanckenhorn, *Callista (Callista) chione* (Linne). The succession goes further on by a gray mudstone, having a thickness of 12.5 m and interbedded with 10

to 20 cm thick sandstone levels. The next one; 60 cm thick calcareous sandstone has been penetrated to gain Sample Bgt-6, displaying the presence of Gastropoda, *Natica millepunctata* Lamarck. The sequence continues with a parcel, consisting of 70 cm thick mudstone, 2.5 m thick, light gray colored sandy limestone, embracing algal remains and corals, at which base shell accumulation has been met, and over which a 4 m thick mudstone-sandstone alternation.

Exemplified by Sample Bgt-7, the next lithology, the 20 cm thick sandy limestone, including algal remains and corals, exhibits a shell accumulation at the base and also includes Gastropoda, *Clavatula asperulata* (Lamarck). The units lying on that, are mudstone-sandstone alternance, exhibiting a 6.5 m thickness and the sandy limestone, including broken shells, respectively. The Sample Bgt-8 has been collected from the latter and that submits no paleontological form. Continuing on by the 1 m thick mudstone-sandstone and 1 m thick sandy limestone, 40 cm thick and including algae and pebbles, all these lithologies suggests a gradation into a shallow-water from relatively deep waters. The capping lithologies are 14 m thick sandstone, comprising limestone and mudstone interbeddings occasionally, 1 m thick sandstone, with gravels scattered throughout and the 40 m thick polygenic conglomerate, that is made up of poorly sorted and angular limestone and ophiolite pebbles. The sequence is covered tectonically by the lowermost slab of the Lycian nappes, the Dumanlıdağ nappe.

Through the section, coarsening in grain-size upwardly, increasing in sand percentage while the mudstone and claystone dominate the lower parts, presence of algal and coral

reef limestones within the succession and introducing to conglomerate, all these imply a regression.

b) Akçasupınarı section characterizes Uçarsu formation, at the base of which rests conformably upon the Elmalı formation (Fig. 3). The section generally consists of mudstone-sandstone alternation. The sample numbered Ak-1, picked up at around 30 m, contains Gastropoda, *Turritella terebralis turritissima* Sacco, *Turritella terebralis subagibbosa* Sacco, *Turritella (Turritella) turris* Basterot, *Turritella (Haustator) striatellatus* Sacco, *Turritella (Haustator) tricincta* (Borson), *Turritella (Peyrotia) desmarestina* Basterot, *Turritella (Zaria) subangulata* (Brocchi), *Conus conoponderosus* (Sacco), Scaphopoda, *Dentalium (Antalis) cf. bouei* Deshayes and Bivalvia, *Anadara (Anadara) diluvii* (Lamarck), *Glycymeris pilosa deshayesi* (Mayer), *Glycymeris (Glycymeris) cor* (Lamarck), *Pitar (Paradione) lilacinoidea* (Schaffer), *Callista (Callista) chione* (Linne).

The other sample numbered Ak-2 has been taken from the sandy limestone at 140 m and embraces Gastropoda, *Turritella (Peyrotia) desmarestina* Basterot, *Xenophora deshayesi* (Michelotti), *Ancilla (Baryspira) glandiformis* (Lamarck), *Ancilla (Baryspira) obsoleta* (Brocchi), *Clavatula asperulata* (Lamarck) and Bivalvia, *Anadara (Anadara) diluvii* (Lamarck), *Glycymeris (Glycymeris) inflatus* (Brocchi), *Cardium praeaculeatum* Holzl, *Venus (Antigona) burdigalensis producta* Schaffer, *Pitar (Paradione) lilacinoidea* (Schaffer), *Callista (Callista) chione* DeFrance.

c) At the base of Uçarsu section, Uçarsu formation rests unconformably upon the Elmalı formation (Fig. 4). The formation initiates with the 70 cm thick, greenish gray colored sandy mudstone, containing poorly sorted

and ill-rounded pebbles-gravels scattered throughout. The Sample Uç-1 from that basal portion possesses Gastropoda, *Turritella terebralis turritissima* Sacco, *Turritella terebralis subagibbosa* Sacco. The greenish gray colored sandstone-mudstone alternation having 4.5 m thickness sits on that lithology. The following rock-type is 1 m thick, brown colored sandstone from which Sample Ug-2 was gathered. That sample contains Gastropoda, *Turritella terebralis* Lamarck, *Turritella terebralis subagibbosa* Sacco and nannoplanktons, *Toweius gammation* (Bramlette-Sullivan), *Coccolithus miopelagicus* Bukry, *Cyclonolites abisectus* (Muller) depicting a Miocene age (determined by Karakullukçu, H.).

Sample Ug-4 is devoid of any fossil form and the Sample Ug-5 includes planktonic foraminifera, *Globigerinoides altiapertura* Bolli, *Globigerinoides trilobus trilobus* (Reuss), *Globigerinoides cf. bisphericus* Todd, giving Upper Burdigalian age (determination by Hakyemez, A.). The sequence goes further on by 32 m thick, gray colored mudstone and again a 8 m thick, gray colored mudstone. Sample Ug-6 from the uppermost of underlying and Sample Ug-7 from the overlying lithologies respectively, holds Upper-Burdigalian aged *Catapsydrax unicavus* Bolli, Loeblich and Tappan, *Globigerinoides trilobus trilobus* (Reuss) and *Globorotalia* sp. forms (determined by Hakyemez, A.).

Sample Ug-8, taken from greenish gray colored mudstone involves Gastropoda, *Turbonilla (Mormula) aturensis* (Cossmann and Peyrot), *Natica millepunctata* Lamarck, *Ficus (Ficus) geometra* (Borson), *Clavatula asperulata* (Lamarck), and Bivalvia, *Anadara (Anadara) fichteli* (Deshayes), *Glycymeris (Glycymeris) bimaculatus* (Poli), *Pecten* sp. and besides those, an ahermatype coral,

Acanthocyathus versicostatus (Michelin), giving Upper Burdigalian-Langhian age (determined by Babayiğit, S.).

The blanketing 6 m thick mudstone comprises 50 to 100 cm thick reef limestone lenticules, including increasingly algae and corals. The concealing, 1.5 m thick, gray colored mudstone exhibits a sandstone lenticule and examination of the Sample Ug-9 from that lithology has displayed the presence of Gastropoda, *Turritella (Turritella) turns* Basterot and *Bivalvia, Venus (Ventricoloidea) multilamella* (Lamarck). Another finding from that is *Catapsydrax dissimilis* (Cushman), claiming a Burdigalian age (determination by Hakyemez, A.).

d) Siradona section has been commenced with polygenic conglomerate, 6 m thick, having grain-matrix and of which pebbles-gravels are angular, moderately and/or well cemented, poorly sorted and displaying normal grading (Fig. 5). This rock-type rests unconformably upon the Elmalı Formation. The following 3 m thick and gray-green colored conglomerate (pebblestone)-sandstone-mudstone alternation pictures medium-layering and is underlain by 2.3 m thick, green colored mudstone. The sample numbered S-1 from that contains Gastropoda, *Turritella terebralis turritissima* Sacco, *Turritella terebralis subagibbosa* Sacco and *Subula (Oxymeris) plicaria* (Basterot).

Through the testing of Sample S-2 from the uppermost part of mudstone, the Gastropoda, *Turritella terebralis turritissima* Sacco has been encountered.

The capping lithology is 34 m thick, greenish gray colored mudstone, bearing thin claystone interbeddings and of which bedding planes are invisible. At 9.5 m of that lithology the samples S-3 and S-4 were gathered to-

gether. By reviewing these samples, the Gastropoda, *Turritella (Turritella) turns* Basterot, *Turritella (Archimediella) bicarinata* (Eichwald), Scaphopoda, *Dentalium (Antalis) cf. bouei* Deshayes and nannoplanktons, *Cyclacargolithus abisectus* (Muller), *Helicosphaera kamptneri* Hay-Mohler, *Sphenolithus belemnos* Bramlette-Wilcoxan, *Sphenolithus delphix* Bukry, *Sphenolithus predistentus* Bramlette-Wilcoxan, *Ericsonia formosa* (Kamptner), *Dictyococcites bisectus* (Hay-Mohler-Wade), *Discoaster deflandrei* Bramlette-Riedel, *Chiasmolithus gigas* (Bramlette-Sullivan), *Reticulofenestra* sp., *Pontoshaera* sp., and *Rhabdosphaera* sp., giving Lower Miocene age, were found (determined by Karakullukçu, H.).

The Sample S-5 from 60 m thick mudstone embraces *Cypfaea (Bernaya) fabagina* (Lamarck), belonging to Gastropoda. Continuing upward with an alternation of mudstone and reef limestone, in the rest of the section no mollusc form has been encountered to obtain age determination. Reef limestones contain algae and corals. Upward coarsening of the grain size has been considered as a clue for the rapid shallowing. The sequence terminates with the ophiolite pebbles-gravels. The whole succession is capped tectonically by Dumanlıdağ nappe, a constituent of Lycian nappes.

Depositional Environment. - The formation represents a transgressive shallow marine setting at initial stages and includes tropical-subtropical molluscs. Over the time, the environment has increasingly deepened and ahermatypic corals and planktonic foraminifera were become plentiful. Seemingly, the environment has intensely shallowed later on. The upper intervals of the formation consist of coarse pebbles and gravels throughly. According to Şenel et al., 1989, causal effect for the

regression and variation in grain size has been the approach and emplacement of the Lycian nappes. By that view, it could be concluded that the thrust movements have been effective toward the end of Upper Burdigalian throughout the region.

Kasaba formation

Description.- Rathur, 1967 and Zaralıoğlu, 1967 had described all Miocene aged rock-units within the region as Kasaba formation. Önalın, 1979 has restrained the unit, subdividing it into two. That researcher has called the Burdigalian-aged units as Sinekci formation and that has considered the ones recording Helvetian-Tortonian age as Kasaba formation, Helvetian-Tortonian in age. Şenel et al., 1989 have claimed that Kasaba formation has been observed within Beydağları autochthon and so reexamined its extension.

Type locality.- Ortabağ township at Kasaba plain.

Localities of the sections.- Ardıılıburun, Dikenlialan stream, Çamköy, Ortabağ and Boyacıpman.

Contact relationships.- Kasaba formation rests unconformably upon the Beydağları formation and Kıbrısdere and Gömüce members of the Sinekçi formation, although it covers the Çayboğazı member of Sinekçi formation conformably. Toward northwestern it is underlain technically by Elmalı formation, involving in the Gömbe group of Yeşilbarak nappe, while at Sidek plain in southeast, Felenkdağ conglomerate overlies it with an unconformity.

Lithology.- The formation consists of thick-layered polygenic conglomerate (pebblestone), light gray, brownish-greenish gray and yellow colored sandstone-mudstone and intercalated reef limestone lenticules.

In Boyacıpman section, the formation initiates with the claystones, 3 m thick and bearing thin sandstone and clayey sandstone beds occasionally. The overlying mollusc-rich sandstone suggests shallowing. Toward the upper sect, that rock-type alternates with the sandy limestone and mudstone. The succession comes to an end with a thick conglomerate, reaching to 8 m.

The Ortabağ section begins with the green colored claystone, 3 m thick and bearing greenish gray colored and 5-15 cm thick sandstone layers occasionally. On that, 1 m thick, gray-green colored gravelly-sandy mudstone is observed. The 2 m thick conglomerate, that is gray colored and made up of rounded and poorly sorted pebbles-gravels covers that. Going further on by muddy-gravelly sandstone, the succession terminates with the conglomerate.

Thickness.- The thickness varies between 0 and 200 meters.

Fossil content and age.- The species *Divaricella ornata subornata* Hilber and *Cerithium zejsneri* Pusch, found through the section, are peculiar to the Lower Badenian stage of central Paratethys. Moreover, it is known that several species, introduced in the formation are also included in marine Lower Badenian stage of central Paratethys. Thus, for the investigation area, the ages Langhian and Lower Badenian, that is contemporary with the former were demonstrated too. The formation has been determined as characterizing that time interval (Table 1). The ages acquiring from the corals, benthic foraminifera and nanoplanktons, found in also support that establishment. The species and the levels at which they were captured through the section has been explained in the following lines.

a- Boyacıpınarı section is characterized by a 3 m thick, green colored claystone, bearing thin sandstone and clayey sandstone interbeddings (Fig. 6). Sample Fd-1a at that level contains Gastropoda, *Bulla* sp., *Bivalvia*, *Corbula (Varicorbula) gibba* (Olivi) and Mioocene-aged nannoplanktons, *Helicosphaera kamptneri* Hay-Mohler, *Coccolithus miopelagicus* Bukry, *Sphenolithus conicus* Bukry, *Cyclicargolithus abisectus* (Muller), *Cyclicargolithus floridanus* (Roth-Hay), *Dictyococcites bisectus* (Hay-Mohler-Wade) and *Toweius gammation* (Bramlette-Sullivan) (determined by Karakullukçu, H.). By those specimens, the environment is suggested as being at offshore and deeply waters of open shelf.

The following rock-type is the 50 cm thick, gray-green colored clayey sandstone, bearing *Operculina* sp. That is underlain by 1.2 m thick, medium-bedded, greenish gray colored and fine-grained sandstone. Changing in lithology reflects becoming shallower increasingly. The Sample Fd-1, gained from that sandstone exhibits Gastropoda, *Ancilla (Bayspira) glandiformis* (Lamarck), *Conus (Conolithus) dujardini* Deshayes and *Bivalvia, Lutraria (Psammophila) oblonga* Chemnitz.

The next one, sampled by Fd-2, is 1 m thick and green colored, molluscs-rich claystone and that bears Gastropoda, *Xenophora deshayesi* (Michelotti), *Strombus (Strombus) bonellii* Brongniart, *Natica millepunctata* Lamarck, *Ancilla (Baryspira) glandiformis* (Lamarck), *Clavatula asperulata* (Lamarck), *Conus (Chelyconus) fuscocingulatus* Bronn, *Subula (Oxymeris) plicaria* (Basterot) and *Bivalvia, Glycymeris pilosa deshayesi* (Mayer), *Nemocardium spondyloides* (Hauer), *Venus (Ventricoloidea) multilamella* (Lamarck), *Callista (Callista) chione* (Linne).

The overlying package consists of a 20 cm thick, gray-green colored sandstone, a 30 cm thick siltstone, bearing *Operculina* sp. abundantly, and a 3 m thick, green colored mudstone, sampled by Fd-3, containing Gastropoda, *Ancilla (Baryspira) glandiformis* (Lamarck), *Clavatula (Clavatula) calcarata francisci* Toulou. The section advances with a 50 cm thick, gray-green colored, fine-grained sandy limestone and a 1.6 m thick, green colored mudstone. The sample numbered Fd-4 from that submits Gastropoda, *Turritella (Turritella) turris* Basterot, *Turritella (Turritella) tricarinata* (Brocchi), *Turritella (Haustator) striatellatus* Sacco, *Ancilla (Baryspira) glandiformis* (Lamarck) and *Bivalvia, Glycymeris pilosa deshayesi* (Mayer) and *Divaricella ornata subornata* Hilber.

Going on through a 2.5 m thick, medium layered sandy limestone, at which the section has been sampled by Sample Fd-5, bearing Gastropoda, *Turritella (Turritella) turris* Basterot, continues with a 60 cm thick, green colored mudstone, overlying that. The upcoming lithologies are 15 m thick, massive sandy limestone, bearing gravels scattered throughout and a 2 m thick, green colored algal mudstone. The Sample Fd-6 from that displays the presence of broken and washed coral fragments, as exemplified by *Tarbellastrea* sp., and algal flocculations (determined by Babayigit, S.). The following lithology in the succession is 60 cm thick, green colored mudstone.

The rock type resting upon that is 17 m thick, gray colored, massive limestone, bearing fine grained sandstone interbeds. Within that, small algae-coral reefs, including bioclastic material and made up of large coral heads and red algae enveloping them are observed. Those reefs lenticulate laterally. The corals constituting the reefs are the ones such

as *Coloria sicilae* Chevalier, *Defrancia irregularis* (Defrane), *Heliastrea tchihatcheffi* Chevalier, *Favia* sp., *Porites* sp. These suggest a Upper Burdigalian-Lower Langhian time interval (determined by Babayiğit, S.). The Sample Fd-7, taken from the covering gray colored sandstones embraces Gastropoda, *Cerithium* (*Therichium*) *europaeum graciliornata* Sacco, *Conus conoponderosus* (Sacco) and *Bivalvia*, *Barbatia* (*Barbatia*) *barbata* (Linne), *Anomia* (*Anomia*) *ephippium rugulosostriata* Bronn, *Pseudochama* (*Pseudochama*) *gryphina taurolunata* (Sacco) and *Venus* (*Ventricoloidea*) *multilamellata* (Lamarck).

The sequence continues with 30 cm thick, green colored claystone and another lithology, 10.5 m thick and gray colored, medium-layered sandstone, from which Sample Fd-8 has been picked up blankets that. That specimen envelopes Gastropoda, *Turritella* (*Archimediella*) *bicarinata* Eichwald, *Turritella* (*Haustator*) *tricincta* (Borson), *Cerithium* (*Pychocherithium*) *turritoplicatum* Sacco, *Cerithium* (*Therichium*) *vulgatum miocenicum* (Vignal), *Clavatula* (*Clavatula*) *calcarata francisci* Toulou and *Bivalvia*, *Pseudochama* (*Pseudochama*) *gryphina taurolunata* (Sacco), *Venus* (*Ventricoloidea*) *multilamella* (Lamarck). Sample Fd-9, taken from the 1 m thick, greenish yellow colored mudstone covering that lithology, contains gastropods, exemplified by *Turritella* (*Turritella*) *turris* Basterot, *Turritella* (*Haustator*) *tricincta* (Borson), *Turritella* (*Archimediella*) *bicarinata* Eichwald, *Cerithium* (*Pychocherithium*) *turritoplicatum* Sacco, *Cerithium zejsneri* Pusch, *Cerithium* (*Therichium*) *vulgatum miocenicum* (Vignal), *Ancilla* (*Baryspira*) *glandiformis* (Lamarck), *Cojnus conoponderosus* (Sacco), *Conus striatulus* Brocchi and bivalves, embodied by *Barbatia* (*Barbatia*) *barbata* (Linne), *Glycymeris pilosa deshayesi* (Mayer), *Glycymeris* (*Glycymeris*)

cor (Lamarck), *Glycymeris* (*Glycymeris*) *inflatus* (Brocchi), *Amusium cristatum* (Bronn), *Venus* (*Ventricoloidea*) *multilamella* (Lamarck) and *Nemocardium spondyloides* (Hauer).

b-Ortabağ section is introduced with approximately 3 m thick, green colored claystone, bearing greenish gray colored sandstone interbeddings, of which thicknesses vary between 5 and 15 centimeters. The Sample Çb-1 from that claystone yields *Turritella* (*Turritella*) *turris* Basterot, *Turritella* (*Archimediella*) *bicarinata* Eichwald, *Aporrheis pespelecani* (Linne), *Natica millepunctata* Lamarck, owing to Gastropoda; *Anadara* (*Anadara*) *diluvii* Lamarck, *Corbula* (*Varicorbula*) *gibba*, the species of *Bivalvia* and *Scaphopoda*, *Dentalium* sp.

The section is extended by 1 m thick, gray-green colored gravelly-sandy mudstone. The Sample Çb-2 from that produces huge amounts of mollusc species, exemplified by gastropods, *Turritella* (*Turritella*) *tricarinata* (Brocchi), *Turritella* (*Turritella*) *turris* Basterot, *Turritella* (*Zaria*) *spirata* (Brocchi), *Turritella* (*Archimediella*) *bicarinata* Eichwald, *Cypraea* (*Bernaya*) *fabagina* Lamarck, *Polinices* (*Polinices*) *redemptus* (Michelotti), *Natica millepunctata* Lamarck, *Distorsio* (*Rhysema*) *tortuosa* (Borson), *Ficus* (*Ficus*) *geometra* (Borson), *Murex* (*Bolinus*) *subtorularius* Hoernes-Auinger, *Galeodes cornutus* (Agassiz), *Laticulus* (*Dolicholaticulus*) *dispar* (Peyrot), *Ancilla* (*Baryspira*) *glandiformis* (Lamarck), *Clavatula asperulata* (Lamarck), *Conus antiquus* Lamarck, *Conus clavatulus* d'Orbigny, *Conus* (*Chelyconus*) *fuscocingulatus* Bronn, *Conus mercati* Brocchi, *Conus* (*Chelyconus*) *puschi* Michelotti, *Subula* (*Oxymeris*) *plicaria* (Basterot); bivalves, exemplified by *Anadara* (*Anadara*) *turonica* (Dujardin), *Glycymeris pilosa deshayesi* (Mayer), *Glycymeris* (*Glycymeris*)

cor Lamarck, *Pecten fuschi* Fontannes, *Pecten (Flabellipecten) solarium* Lamarck, *Pynodonta germanitala* (de Gregorio), *Codokia leonina* (Basterot), *Nemocardium spondyloides* (Hauer), *Nemocardium spondyloides herculeum* Dollfuss-Cotter-Gomez, *Venus (Ventriculoidea) multilamella* (Lamarck), *Callista (Callista) chione* (Linne), *Corbula (Varicorbula) gibba* (Olivi). That sample also surrenders benthic foraminifera, exemplified by *Borelis melo* (Fichtel and Moll), *Amphistegina* sp., *Operculina* sp., implying a Late Burdigalian-Tortonian age (determined by Sirel, E.). By faunal assemblage it has been inferred that, that environment was shallower than the former and represented the shallow parts of the shelf.

Depositional environment-Mollusca-rich Kasaba formation pictures a subtropical climate and shallow parts of the shelf. Diversification in species implies that the environment has unchanged over a long time. It is thought that, the grain-size coarsening and disappearing of the fossil records afterwards have resulted from the moving in of Lycian nappes and regression, due to that approaching.

CONCLUSIONS AND DISCUSSION

Uçarsu and Kasaba formations, which have been examined for mollusc-contents, are observed within different tectonic units. For the ages and environmental characteristics of these units, different persuasions have been proposed. By those,

1. Overlooking the paleogeographic and chronostratigraphic denotations of the species, it has concluded that, several are the ones found in Lower and Middle Miocene marine stages of both Mediterranean Tethys and central Paratethys. *Divaricella ornata subornata* Hilber and *Cerithium zejsneri* Pusch, en-

countered in Kasaba formation, are the species peculiar to Lower Badenian stage and Pitar (*Paradione*) *lilacinoides* (Schaffer) can only be seen in Eggenburgian stage of the central Paratethys. These species, may not be come across in Burdigalian and Langhian stages, are the ones distinguishing Tethyan-fauna-rich central Paratethyan stages (Eggenburgian and Lower Badenian) from Mediterranean Tethyan stages. Therefore, for the investigation area, Eggenburgian-Carpathian-Lower Badenian marine stages of central Paratethys have pictured along with the Upper Burdigalian-Langhian with which the former ones are contemporaneous.

2. None of the species included in Uçarsu formation, *Cassidaria tauropomum* (Sacco), *Vexillum (Uromitra) pluricostata percostulata* (Sacco), *Pecten zizinae* Blanckenhorn, *Chlamys (Macrochlamys) latissima praecedens* (Sacco), *Pitar (Paradione) lilacinoides* (Schaffer), *Cardium praeculeatum* Hölzl, *Venus (Antigona) burdigalensis producta* Schaffer, *Turritella terebralis turritissima* Sacco, *Turritella (Peyrotia) desmarestina* Basterot, characterizing Lower Miocene could be registered in Kasaba formation, while the ones, found in Kasaba formation, namely *Divaricella ornata subornata* Hilber and *Cerithium zejsneri* Pusch proper to Lower Badenian, can not be observed in Uçarsu formation. Thus, these two formations are not contemporary and those developed in different periods, following one another.

3. Poisson, 1977 has claimed that the green colored marl, including levels with *Operculina* sp. at lowermost part of the Kasaba formation is Upper Burdigalian in age and the overlying marl and conglomerate represents the Langhian stage and he also has proposed a Serravallian time duration for the following parts of that section. Hayward

(1982, 1984), has emphasized that the Kasaba formation is Upper Miocene in age and that unit depicts a fan-delta, picturing a regressive marine sequence terminated with the alluvial fan systems. Şenel et al., 1989 has stressed that, Kasaba formation typifies a Upper Burdigalian-Lower Langhian duration and that has undergone the tectonic movements. Tuzcu et al. (1994) have also proposed that the formation characterizes a Upper Burdigalian-Lower Langhian time interval. For the author of the text, by the context of mollusk-fauna, Kasaba formation deposited at a warm and shallow marine environment and that implies a regressive succession, giving a Langhian (Lower Badenian) age.

4. The age of the Uçarsu formation has previously been considered as Upper Burdigalian-Lower Langhian by Şenel et al. (1989,1994) and Tuzcu et al. (1994) although it has been concluded as Upper Burdigalian (Upper Eggenburgian-Carpathian) through this investigation, by the molluscs determined. Planktonic foraminifer and nannoplankton findings also uphold that approach. Uçarsu formation offers a sequential development, introduced with transgressive levels and comes up to an end through regressive character. On the contrary, Kasaba formation submits a Langhian (Lower Badenian) duration, by the presence of *Divaricella ornata subornata* Hilber and *Cerithium zejsneri* Pusch, appearing at the initiation of Middle Miocene, These forms, as specified previously, are proper to Lower Badenian too.

5. It is known that at the region the Lycian nappes had firstly lodged and then the Yeşilbarak nappe had been fallen beneath those. All these have overlain the Lower-Middle Miocene aged units technically (Poisson, 1977; Önal, 1979; Şenel et al., 1989,1991, 1992, 1994; Şenel, 1997). The duration of

those emplacements have been estimated as Langhian by Poisson, 1977 though considered as Lower Langhian by Şenel et al. (1987, 1989, 1991, 1992, 1994) and Şenel 1997 a,b,c. But it might undeniably be clarified through the search that, the Nappes had begun effective toward the end of Upper Burdigalian and that phenomena continued until the closure of Langhian, as attested by the paleontological findings in both formations and stratigraphic relationships.

ACKNOWLEDGMENT

That research comprises part of "Ph. D. Thesis", has been performed at Department of Geology, Faculty of Sciences, Ankara University. The authors would kindly respect to authorities of General Directorate of MTA for their supports in field surveying and laboratory examinations, to executive committee of TÜBİTAK since their helps in having a scholarship abroad, coded NATO-A2, to Dr Mustafa Şenel for his helpful efforts in the studies performed at field and office, to Dr Margit Bohn-Havas for paving the way for examinations at Natural History Museum of Hungary and Geological Institute of Hungary, to Dr Ortwin Shultz because of leading to have opportunity for benefits from Natural History Museum of Austria, to Dr Alfred Dulai for the courtesy of his special collection at Natural History Museum of Hungary, to Aynur Hakyemez at MTA for determinations of planktonic foraminifera, to Hatice Karakullukçu (MTA), since determinations of nannoplanktons, to Sedef Babayiğit (MTA) for descriptions of the corals and to Dr Ercüment Sirel (AU) for descriptions of benthic foraminifera and for fruitful criticism on manuscript to Ergun Akay (MTA) and Dr. Kaan Tekin (HÜ).

Manuscript received November 28, 2001

REFERENCES

- Akay, E., Uysal, Ş., Poisson, A., Cravette, Y., and Muller, C. 1985, Antalya Neojen Havzası'nın stratigrafisi: TJK Bull., 28, 105-09
- Bölükbaşı, A.S., 1987, Elmalı (Antalya) - Acıgöl (Burdur) - Korkuteli (Antalya) arasında kalan Elmalı naplarının jeolojisi: TPAO Rep. Num.: 241, 247 p.
- Brunn, J. H., Dumont, J. F., Graciansky, P. Ch. de, Gutnic, M., Juteau, Th., Marcoux, J., Monod, O. and Poisson, A., 1971, Outline of the geology of the western Taurids, Geology and History of Turkey: Petroleum Exploration Society of Libya, Tripoli
- Colin, H., 1955, Jeolojik harita izahnameleri, Elmalı 123/3, 123/4, Kaş 140/1-3 ve Kaş 140/2: MTA Rep. 2246 (unpublished), Ankara
- , 1962, Fethiye-Alanya-Kaş-Finike (GB Anadolu) bölgesinde yapılan jeolojik etütler: MTA Bull., 59, 19-61
- Erakman, B.; Meşhur, M.; Gül, M. A.; Alkan, H.; Özataş, Y. and Akpınar, M., 1982, Fethiye-Köyceğiz-Tefenni-Elmalı-Kalkan arasında kalan alanın jeolojisi. Turkey 6th Petrol Congress, Proceedings, 23-31, Ankara
- Flugel, H., 1961, Isparta 106/3 ve Elmalı 123/1 paftalarının dahilinde yapılan jeolojik löve çalışmaları: MTA Rep. 2372 (unpublished), Ankara
- Günay, Y.; Bölükbaşı, A. S. and Yoldemir, O., 1982, Beydağlarının stratigrafisi ve yapısı: Turkey 6th Petrol Congress Proceedings, Nisan 1982, 90-101, Ankara
- Hayward, A. B., 1982, Türkiye'nin güneybatısındaki Beydağları ve Susuzdağ masiflerinde Miyosen yaşlı kırıntılı tortulların stratigrafisi: TJK Bull., 25(2), 81-89
- , 1984, Miocene clastic sedimentation related to emplacement of the Lycian Nappes and Antalya Complex, SW Turkey (in Geological Evolution of the Eastern Mediterranean Tethys, eds. Dixon, J. E. and Robertson, A. H. F.): Spec. Publ. Geol. Soc. London, 17, 287-300
- Hayward, A. B., and Robertson, A. H. F., 1996, Miocene patch reefs from a Mediterranean Tethys marginal terrigenous setting in SW Turkey: SEPM Concepts in Sedimentology and Paleontology, 317-32
- Holzer, H., 1955, GB Anadolu'daki Kaş 140/1, 2 ve 3 paftalarına ait tamamlayıcı malumat: MTA Rep. 2369 (unpublished), Ankara
- İslamoğlu, Y., 2001, Aksu ve Kasaba bölgelerinin mollusk faunası ile Miyosen stratigrafisi (Batı ve Orta Toroslar): Ankara Üniversitesi, Fen Bilimleri Enstitüsü, PhD Thesis, 291 s (unpublished), Ankara
- Kirk, H. M., 1932, Çıralı'ya yapılan istikşaf gezisi: MTA Rep. 242 (unpublished), Ankara
- Lucius, M., 1925, Finike havalisindeki tetkik seyahati (Antalya vilayeti): MTA Rep. 195 (unpublished), Ankara
- Manciewicz, M., 1946, Les piments des roches asphaltiques dans les regions d'Akseki et de Finike (Antalya vilayeti): MTA Rep. 2684 (unpublished), Ankara
- Önal, M., 1979, Elmalı-Kaş (Antalya) arasındaki bölgenin jeolojisi: İÜFF Monografileri, PhD Thesis, 29, 131 s, İstanbul
- Pisoni, C., 1967, Kaş, (Antalya İli) bölgesinin jeolojik etüdü: MTA Bull., 69, 41-49
- Poisson, A., 1977; Recherches geologiques dans les Taurides occidentales (Turquie): L'universite de Paris-Sud (Centre D'Orsay), Thesis, Tome 1, Paris
- Rathur, F., 1967, Etude geologique de la fenetre de Göcek Aygırdağ: Fac. Sci. Univ. Grenoble, Thesis,
- Robertson, A. H. F., 1993, Mesozoic-Tertiary sedimentary and tectonic evolution of Neotethyan carbonate platform, margins and small ocean basin in thi Antalya Complex of SW Turkey: Ass. Sediment., Spec. Pubs, 20,415-65
- Şenel, M., 1997a, 1:250 000 ölçekli Türkiye Jeoloji Haritaları, Fethiye paftası: No 2, MTA, Ankara

- Şenel, M., 1997b, 1:250 000 ölçekli Türkiye Jeoloji Haritaları, Antalya paftası: No 3, MTA, Ankara
- , 1997c, 1:250 000 ölçekli Türkiye Jeoloji Haritaları, Isparta paftası: No 4, MTA, Ankara
- , Arbas, A., Bilgi, C., Bilgin, Z., Dinçer, M.A., Durukan, E., Erkan, M., Karaman, T., Kaymakçı, H., Örçen, S., Selçuk, H. and Şen, M.A., 1986, Gömbe - Akdoğan'ın stratigrafik ve yapısal özellikleri: Kaş- Antalya. Geological Congress of Turkey, Abstracts, 51.
- , Selçuk, H.; Bilgin, Z.; Şen, M. A.; Karaman, T.; Erkan, M.; Kaymakçı, H.; Örçen, S. and Bilgi, C., 1987, Likya Napları ön-cephe özellikleri (GB Türkiye): Geological Congress of Turkey, Abstracts, 6
- , Bilgin, Z.; Şen, M. A.; Karaman, T.; Dinçer, M. A.; Durukan, E.; Arbas, A.; Örçen, S. and Bilgi, C., 1989, Çameli (Denizli)-Yeşilova (Burdur)-Elmalı (Antalya) ve dolayının jeolojisi: MTA Rep. 9429 (unpublished), Ankara
- , Bilgin, Z.; Dalkılıç, H.; Gedik, I.; Serdaroğlu, M.; Uğuz, F. and Korucu, M., 1991, Eğirdir-Sütçüler-Yenişarbademli arası ve yakın dolayının (Batı Toroslar) jeolojisi: MTA Rep. (unpublished), Ankara
- , Dalkılıç, H.; Gedik, I.; Serdaroğlu, M.; Bölükbaşı, S.; Metin, S.; Esentürk, K.; Bilgin, A. Z.; Uğuz, F.; Korucu, M. and Özgül, N., 1992, Eğirdir-Yenişarbademli-Gebiz ve Geriş-Köprülü (Isparta-Antalya) arasında kalan alanın jeolojisi: MTA-TPAO Rep. 3132, 559 s (unpublished), Ankara
- , Akdeniz, N.; Öztürk, E. M.; Özdemir, T.; Kandıncı, G.; Metin, Y.; Öcal, H.; Serdaroğlu, M. and Örçen, S., 1994, Fethiye (Muğla)-Kalkan (Antalya) ve kuzeyinin jeolojisi: MTA Rep. 9761 (unpublished), Ankara
- , and Bölükbaşı, A.S., 1997, 1:100 000 ölçekli Türkiye Jeoloji Haritaları, Fethiye M-9, No 5, MTA, Jeo. Etüt. Dairesi, Ankara.
- Tunoğlu, C. and Bilen, C., 2001, Burdigalian- Langhian (Miocene) ostracod biostratigraphy and chronostratigraphy of the Kasaba basin (Kaş / Antalya), SW Turkey, *Geologica Carpathica*, 52, 4, 247-258.
- Tuzcu, S.; Karabıyıköğlu, M. and İslamoğlu, Y., 1994, Batı Toroslar Miyosen mercan resifleri: Bileşimleri, fasiyes özellikleri, ve ortamsal konumları: 47th Geological Congress of Turkey, Abstracts, s 16
- Yalçınkaya, S., Engin, A., Taner, K., Afşar, Ö. P., Dalkılıç, H. and Özgönül, E., 1986, Batı Torosların jeolojisi: MTA Rep. 7898 (unpublished), Ankara
- Zaraloğlu, M., 1967, Demre-Finike-Çatallar arasında kalan sahanın detay jeolojik etüdü: MTA Rep. 4027 (unpublished), Ankara.

OOLITE AND PISOLITE OCCURRENCE WITHIN THE PLIOCENE - QUATERNARY AGE TRAVERTINE IN MUT REGION

Eşref ATABEY*

ABSTRACT.- There exists oolite and pisolite occurrences within travertine of Pliocene-Quaternary age at north-east of Mut (İçel). The oolite grains are smaller than 2 mm, whereas pisolite grains are between 2 mm and 1 cm in size. These are rounded and ellipsoidal in shape. Each oolite and pisolite grain contains a nucleus at its centre, elastic carbonate sand grain, surrounded by laminated concentric calcite layers. These occurrences developed from roof, mixing grains in the splashing pool.

LITHOSTRATIGRAPHY AND FACIES CHARACTERISTICS OF THE CONTINENTAL - SHALLOW - MARINE
MIOCENE DEPOSITS (ZARA - SİVAS)

Erdal KOŞUN** and Attila ÇİNER***

ABSTRACT.- The and space relationships of sedimentary environments and depositional evolution of Sivas Miocene Basin is studied south of Zara town. 2 formations and 4 members are defined. Early Miocene Ağılkaya formation (1900 m) is composed of Karayün member (alluvial fan and fluvial deposits), Hafik member (sabkhaic gypsums) and Karacaören member (shallow marine). On the other hand Early-Middle Miocene Eğribucak formation (550 m) is only represented by Sekitarla member (fluvial deposits) in this part of the basin. Facies analyses reveal 13 lithofacies representing deposition in lagoon to shallow marine, tidal flat, playa and sabkha, alluvial fan and fluvial environments. The currently debated and controversial relative age of the Hafik member gypsum deposits is assigned to (?) Oligocene - Early Miocene based on the stratigraphic relations observed throughout the basin. Petrographic data together with North-Northwestern paleocurrent directions indicate an ophiolitic source area situated to the South-Southeast of the basin.

LATE PLIOCENE PELECYPODA AND GASTROPODA CONTENT AND STRATIGRAPHY OF THE DATÇA PENINSULA (MUĞLA - SW ANATOLIA)

Sevinç Kapan YEŞİLYURT* and Güler TANER*

ABSTRACT.- This study examined the paleontology and stratigraphy of the Neogene rock units exposed around Datça Peninsula basing on the pelecypoda and gastropoda fauna. One of the fossil specimens (*Hydrobia tanerae* n.sp.) which are determined from the taken measured stratigraphic sections belonging to Yıldırımli formation was described as a new species. The age of Neogene units in the investigated area is determinal as Late Piacencian with the pelecypoda and gastropoda fauna. According to these marine and fresh water fauna, it is found that the area was a lagoon in Late Piacencian. ESR (Electron Spin Resonance) Age Method was applied on the four fossil specimens and found 1.891-1.988 million years. This result supported the Late Piacencian age.

CLAY MINERALIZATION IN HYDROTHERMALLY ALTERED TEKKE VOLCANICS (ÇUBUK, ANKARA NE)

Asuman BESBELLI*** and Baki VAROL****

ABSTRACT.- The Neogene volcanics represented by andesites, andestitic tuffs and trachy-andesites in the north-east of Ankara contain hydrothermally altered clay mineralization in places. In the alteration zones developed in the areas where the hydrothermal fluids leaking along faults and joints alter volcanic rocks, silicifications and iron oxides and sulfides are observed next to the clays minerals. As a result of alteration starting from the unaltered rocks, different zones poor in clay and silicified have been developed. In this aspect various petrographic types have been distinguished in the form of unaltered volcanic rocks, volcanic rocks poor in alteration, highly altered volcanic rock and silicified rocks. In addition, gold has been found in the samples around Gıcık. The clay minerals formed as a result of hydrothermal alteration of the Neogene volcanics have been determined as kaolinite, montmorillonite and illite, the silicate minerals as quartz and cristobalite, and ferrous compounds as pyrite, very little calcopyrite, hematite, lepidoclorite and goethite. Kaolinization has generally been observed around the Gıcık village and Ilgaz hill, smecticization around the Kurtsivrisi village, and illitization in both regions. Their zonation has been developed in the form of kaolinite, montmorillonite and illite from the inner zone which is nearest the fault, montmorillonite and illite have been formed in the more outer zone. In the fluid inclusion studies carried out, the homogenization heat of quartz has been found to be between 170 °C and 140 °C. This datum shows that the clay mineralization due to alteration within the volcanic rocks has been realized under epithermal conditions. However, the presence of gold in the environment makes us think that the hydrothermal solutions coming from the magma have also been effective in the alteration in addition to the main factor, the meteoric waters.